7-27-2016 12:00 AM

Temperature-dependent alterations of brown adipose tissue metabolism during hibernation in the thirteen-lined ground squirrel, *Ictidomys tridecemlineatus*.

Sarah V. McFarlane
The University of Western Ontario

Supervisor
James F. Staples
The University of Western Ontario

ABSTRACT

Brown adipose tissue (BAT) is the major thermogenic tissue in small eutherian mammals. In hibernators, seasonal modifications of BAT are well documented but little is known about its functional regulation during hibernation. BAT metabolism is activated by sympathetic stimulation, so I hypothesized that further regulation at the mitochondrial level, as seen in other hibernator tissues, would be of little advantage. Contrary to my predictions, respiration rates of BAT mitochondria isolated from torpid thirteen-lined ground squirrels were suppressed by up to 62% compared with rates from individuals that aroused to interbout euthermia (IBE), when measured at 37°C. At 10°C, however, these rates did not differ between torpor and IBE. Contrary to these results, activities of electron transport system enzymes and brown adipocyte respiration did not differ between torpor and IBE, regardless of assay temperature. The data suggest that BAT mitochondria become less temperature sensitive during torpor, allowing sustained function at low body temperatures.

Keywords: uncoupled thermogenesis, Q_{10}, electron transport system, hibernation, mitochondria, high resolution respirometry, thirteen-lined ground squirrel

CO-AUTHORSHIP STATEMENT

McFarlane, S.V., Mathers, K.E., Staples, J.F. Reversible temperature-dependent alterations of brown adipose tissue mitochondrial respiration during torpor in a mammalian hibernator. (Submitted)

KE Mathers:
- For providing training and assistance with spectrophotometric assays, animal trapping, care and surgery.

JF Staples:
- Principal investigator
- Consultation on experimental design and methods
- Manuscript revisions

EPIGRAPH

We keep moving forward, opening new doors, and doing new things, because we're curious and curiosity keeps leading us down new paths.

- Walter Elias Disney

ACKNOWLEDGEMENTS

TABLE OF CONTENTS

Page

LIST OF TABLES

LIST OF FIGURES

LIST OF APPENDICES

LIST OF ABBREVIATIONS AND SYMBOLS

16:1	palmitoleic acid
ATGL	adipose triglyceride lipase
BAT	brown adipose tissue
BSA	bovine serum albumin
cAMP	cyclic adenosine monophosphate
CAT	carnitine acylcarnitine transferase
CL	cardiolipin
CPT1	carnitine palmitoyltransferase-1
CPT2	carnitine palmytoyltransferase-2
EGTA	ethylene glycol tetraacetic acid
ETS	electron transport system
HB	homogenization buffer
HEPES	4-2(2-hydroxyethyl)-1-piperazineethanesulfonic acid
HSL	hormone sensitive lipase
IBE	interbout euthermia
IMM	inner mitochondrial membrane
IMS	intermembrane space
LA	linoleic acid
MR	metabolic rate
NE	norepinephrine
OMM	outer mitochondrial membrane

PKA   protein kinase A

PLA   phospholipase A

PMF   proton motive force

Q$_{10}$ temperature sensitivity coefficient of a specific biological
                process

SERCA   sarcoplasmic reticulum Ca^{2+}-ATPase 2a

T$_a$ ambient temperature

T$_b$ core body temperature

TNZ   thermoneutral zone

T$_{set}$ thermoregulatory set point

UCP1   uncoupling protein 1

CHAPTER 1

INTRODUCTION

1.1 Animals, environmental pressures, and thermal strategies

The ability of animals to maintain homeostasis can be challenged by their changing environments. One of the most influential abiotic parameters of these environments is fluctuating ambient temperature (T_a). As the temperature at which biochemical reactions occur increases, the rate of reactions also tend to increase (Hochachka and Somero, 2002), and this can be modelled by the Q_{10} effect. With a 10°C increase in reaction temperature, the rate of most enzyme catalyzed reactions typically increase 2-3 fold. This temperature dependence of biochemical reactions poses one of the strongest selective pressures on animals in their changing environments, especially because the vast majority of animal species are ectotherms.

Ectotherms produce and retain little metabolic heat and thus use external sources of heat and behavioral adjustments to regulate their body temperature (T_b). As with biochemical reactions, the metabolic rate (MR) of ectotherms tends to vary with their T_b, following similar Q_{10} patterns (Scholander et al., 1953). Despite their lack of ability to use metabolic heat to defend a constant T_b, some ectotherms still manage to survive in thermal extremes by exhibiting acclimatory responses and thermoregulatory behaviors. Although ectotherms must withstand large changes in T_b, this thermal strategy comes with a very low energetic demand which can be favourable in many environments where energy sources, such as food, are scarce. But ectotherms are not alone in their ability to thrive in energy-

1

poor, thermally-challenging environments. Endotherms produce and retain

significant quantities of metabolic heat, allowing them to defend a constant T_b

even when T_a is very low. A constant T_b allows endotherms to maintain

favourable, predictable conditions for their biochemical reactions, even in

thermally challenging environments. Though this strategy has many benefits, it is

very energetically costly. Compared with similarly-sized reptiles, mammals

exhibit four to eight fold higher metabolic rates, even at the same T_b of 37°C

(Else and Hulbert, 1981; Hemmingsen, 1960). This high metabolic demand

requires mammals to consume far more food energy than their ectothermic

counterparts even when T_a is favourable. This high energetic demand can be even

more challenging to endotherms when T_a fluctuates outside the thermoneutral

zone (TNZ), a species-specific range of T_a that requires minimal metabolic heat

production or evaporative heat loss to maintain T_b. As T_a falls below the lower

critical temperature of this range, mammals must increase metabolic heat

production to regulate T_b, thus increasing MR and the requirement for food

consumption (Kleiber, 1961; Pearson, 1947).

During winter in temperate and polar regions, low T_a and short

photoperiod are associated with low environmental energy availability. Some

animals avoid these environments by migrating, expending energy to relocate to

an environment where food is not limiting and the T_a is within a range that

requires less energy expenditure to maintain T_b. Many small endotherms,

however, do not migrate. Some build food caches in the summer to prepare for

scarce winter resources or constantly forage in these unfavourable conditions,

which can be very energetically costly. Moreover, small mammals have a high surface area to volume ratio, so heat loss in cold T_a is a major hindrance to maintaining a constant (and relatively warm) T_b. To overcome this obstacle, some small mammals greatly increase their metabolic heat production and insulation, expending large amounts of energy in environments where food is already limited. Other mammals have evolved mechanisms, such as hibernation, to reduce energy expenditure in high-energy demanding environments.

Hibernation is characterized by periodic and profound suppression of metabolic rate and T_b, usually during the winter months when T_a is low. Many mammals experience hibernation, including some monotremes and marsupials, and it is believed that hibernation is an ancestral phenotype that has been lost in homeothermy (Lovegrove, 2012). Hibernation has been well-studied in species such as the thirteen-lined ground squirrel (*Ictidomys tridecemlineatus*), an obligate hibernator. The thirteen-lined ground squirrel is widely distributed across the prairies and grasslands of North America and ranges from central Canada to the southern United States. This species copes with the energetic challenge of winter by hibernating from mid-autumn through early spring. Their hibernation season is characterized by recurrent torpor bouts that are spontaneously interrupted by short periods of euthermia every 7-12 days (Fig. 1.1). The transitions between torpor and spontaneous arousals can be described in four phases; arousal, interbout euthermia (IBE), entrance, and torpor. During arousal, MR increases by over 20-fold and T_b rises from 5°C to ~37°C within a few hours. This period of IBE is maintained for as long as 12 hours. Entrance back into

torpor is characterized by a rapid and significant suppression of MR, and a

consequential decrease in T_b into the torpor phase (Fig. 1.2, Brown et al., 2013).
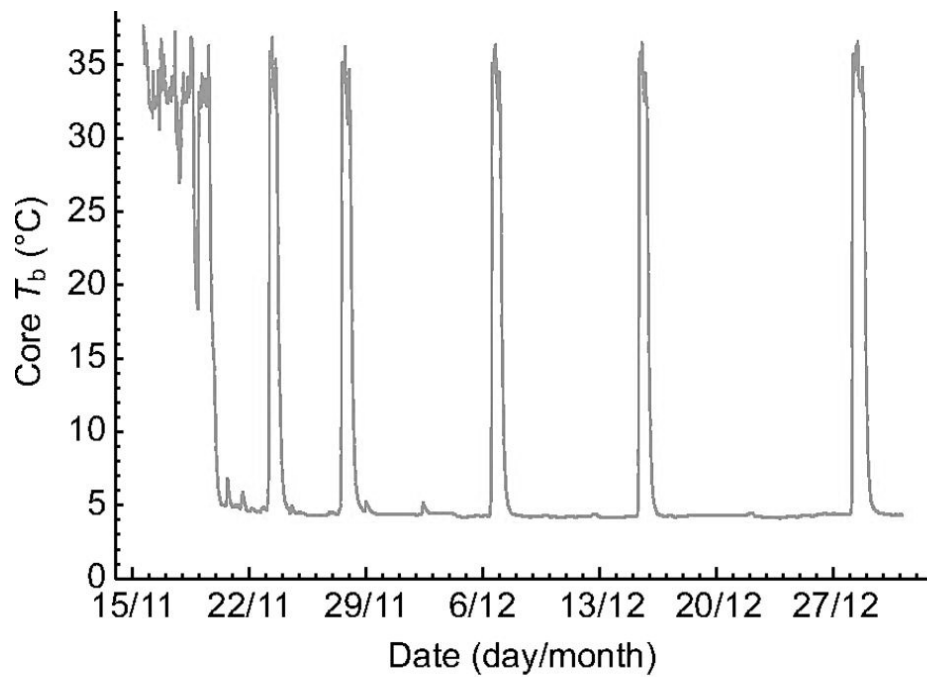
Figure 1.1 Core body temperature (T_b) of a hibernating thirteen-lined ground squirrel (*Ictidomys tridecemlineatus*) over time. This figure shows several torpor bouts ($T_b \sim 5°C$) interrupted by spontaneous arousals to periods of interbout euthermia ($T_b \sim 37°C$). Core body temperature measurements were made using temperature sensitive radio telemeters implanted intraperitoneally. Modified from Staples (2014).
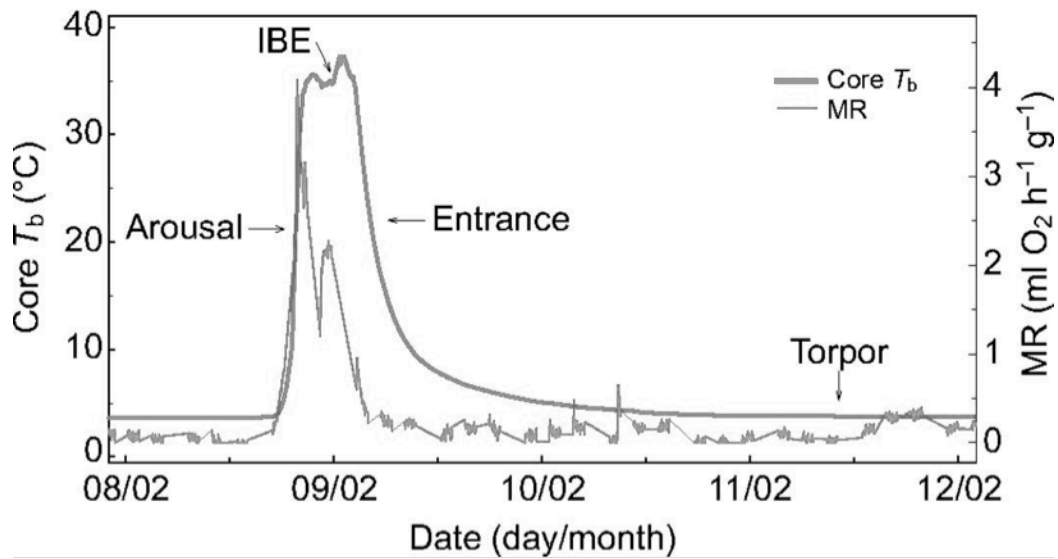
Figure 1.2 Synchronized measurements of core body temperature (T$_b$) and mass-specific whole-animal metabolic rate (MR) of a thirteen-lined ground squirrel (*Ictidomys tridecemlineatus*) in different phases of hibernation. This figure shows the T$_b$ and simultaneous MR of one animal as it transitions from torpor into IBE. During arousal MR increases by over 20-fold and T$_b$ rises from 5°C to ~37°C within a few hours. IBE is maintained for up to 12 hours. Entrance back into torpor is characterized by a suppression of MR and a consequential decrease in T$_b$. Core T$_b$ measurements were made using temperature sensitive radio telemeters implanted intraperitoneally and MR was measured via flow-through respirometry. Modified from Staples (2014).

1.2 Brown adipose tissue and mitochondrial metabolism in hibernation

In hibernators, such as the thirteen-lined ground squirrel, the rapid increase in T_b during arousal from torpor to IBE is realized largely through activation of brown adipose tissue (BAT) located near the cervical and axillary regions. In other sciurid hibernators, shivering also occurs during arousal but only contributes slightly to heat production while most of the increase in T_b can be attributed to uncoupled thermogenesis in BAT (Tøien et al. 2001).

BAT is a thermogenic tissue unique to eutherian mammals and, in fairly large mammal species, is usually only maintained in the early stages of life, before the ability to thermoregulate has fully been established. BAT is distributed around the body in distinct "pads" and can be found around the chest (i.e. interscapular and axillary), pelvic regions, and brain (Cannon and Nedergaard, 2004). This tissue contains cells that are densely packed with mitochondria that surround small lipid droplets (Cannon, 1968). In many small mammalian species, BAT remains present throughout life, usually in small volumes, and BAT proliferation can be induced through cold acclimation (Cameron and Smith, 1964).

During entrance into torpor, there is a reduction in the thermoregulatory set-point (T_{set}), a result of signals from the pre-optic anterior hypothalamus with input from the suprachiasmatic nucleus. This drop in T_{set} shifts the lower limit of the TNZ to lower ambient temperatures (Snapp and Heller, 1981) and halts the sympathetic activation of BAT, effectively stopping thermogenesis in this tissue. During arousal from torpor, T_{set} increases towards euthermic levels, so that

ambient temperatures that had been within the TNZ during torpor suddenly become well below the lower limit of the TNZ. As a result, thermogenesis is initiated, resulting in large increases in MR even before T_b increases (Fig. 1.2). During arousal and IBE, BAT likely accounts for a high proportion of whole-animal metabolism (Tøien et al. 2001) but during entrance into torpor, when T_{set} decreases, sympathetic activation of BAT ceases and uncoupled thermogenesis no longer contributes significantly to the whole-animal MR.

BAT activation occurs through a signaling cascade initiated by norepinephrine (NE) release from sympathetic nerves. Upon signals from the suprachiasmatic nucleus and the hypothalamus, the preganglionic sympathetic nerves release acetylcholine in the sympathetic chain, stimulating the postganglionic sympathetic nerves, that innervate BAT, to release NE (Cannon and Nedergaard, 2004). The NE activates β_3-adrenergic G-protein coupled receptors on the plasma membrane of the brown adipocyte. This activation causes the release of a stimulatory G-protein which activates adenylate cyclase (AC). AC converts ATP into cyclic AMP (cAMP), which activates protein kinase A (PKA). In BAT, PKA phosphorylates hormone sensitive lipase (HSL), activating it. HSL and adipose triglyceride lipase (AGTL) initiate fatty acid cleavage from triglycerides stored within brown adipocytes (Fig. 1.3). These free fatty acids are transported across the outer mitochondrial membrane (OMM) as acyl-carnitines, into the intermembrane space (IMS), and eventually lead to the activation of uncoupling protein-1 (UCP1, see below) (Cannon and Nedergaard, 2004).
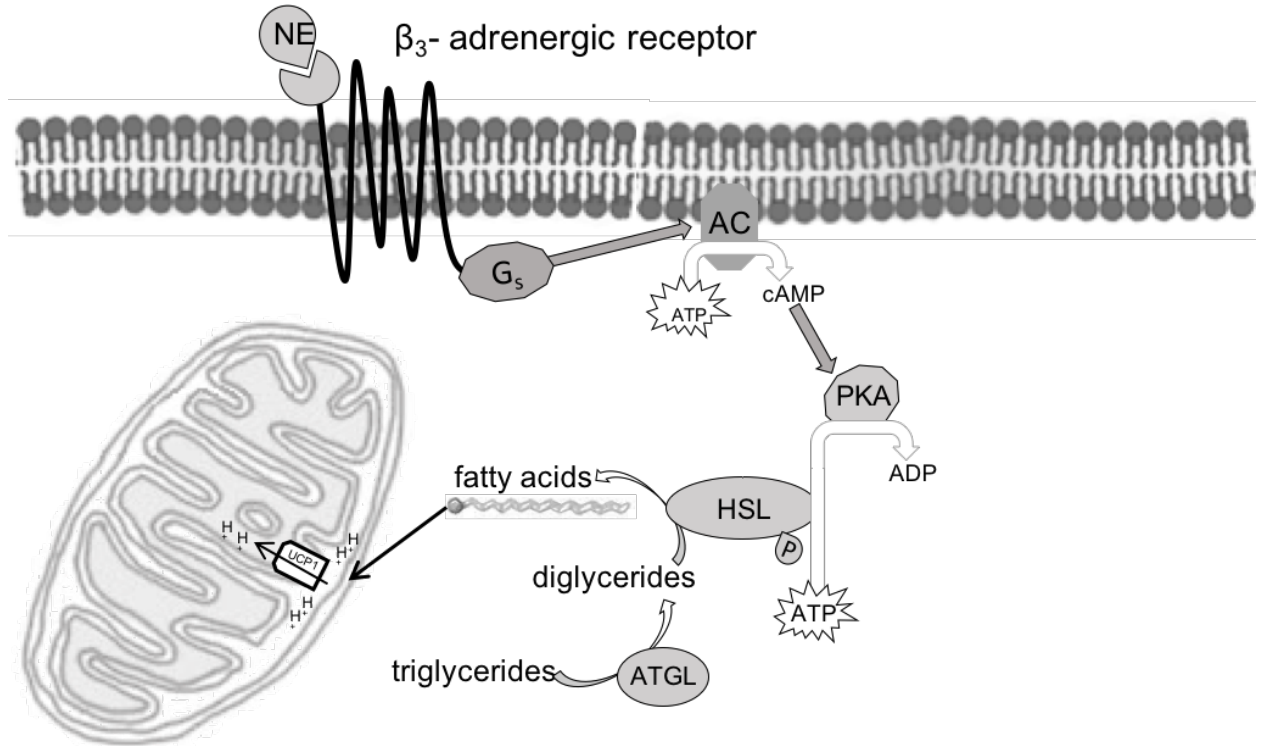
Figure 1.3 Schematic of norepinephrine (NE) initiating a signaling cascade that ultimately leads to the activation of uncoupling protein-1 (UCP1). NE released from the sympathetic nervous system binds to the G-protein coupled β_3-adrenergic receptor. This binding causes the release of stimulatory G-protein (G_s) which activates adenylate cyclase (AC) which converts ATP into cyclic AMP (cAMP). cAMP activates protein kinase A (PKA) which phosphorylates hormone sensitive lipase (HSL). HSL and adipose triglyceride lipase (AGTL) release free fatty acids from intracellular BAT adipocyte triglyceride stores. These free fatty acids are then transported across the outer mitochondrial membrane into the intermembrane space to activate UCP1. This diagram represents work from Cannon and Nedergaard (2004).

In the cytosol of most mammalian cells, including BAT, long chain free fatty acids (released from triglycerides by HSL and ATGL) are converted to fatty acyl-CoAs by an enzyme embedded in the OMM termed long chain acyl-CoA synthetase (Kerner and Hoppel, 2000). The fatty acyl-CoAs subsequently diffuse into the IMS and are transported into the matrix in two steps (McGarry and Brown, 1997). Initially, the enzyme carnitine palmitoyltransferase-1 (CPT1), embedded in the OMM, converts a fatty acyl-CoA and a carnitine into an acyl-carnitine. Next, the acyl-carnitine is transported across the IMM into the matrix by carnitine-acylcarnitine translocase (CAT). Once in the matrix, an enzyme embedded in the inner mitochondrial membrane (IMM), carnitine palmitoyltransferase-2 (CPT2), catalyzes the conversion of the acyl-carnitine into a fatty acyl-CoA, and the released carnitine is transported back across the IMM by CAT (Pande, 1975). In the matrix, the fatty acyl-CoA undergoes β-oxidation to acetyl-CoA, which can enter the Krebs cycle, ultimately producing substrates, such as NADH and succinate, which fuel the electron transport system (ETS) (Fig. 1.4).

Mitochondria provide the chemical energy required for the majority of eukaryotic cellular processes through the production of ATP. ATP production is accomplished by using energy released by substrate oxidation to actively transport protons across the inner mitochondrial membrane (IMM), thus forming an electro-chemical gradient termed the proton motive force (PMF). Formation of the PMF is initiated by ETS oxidation of several substrates including the electron
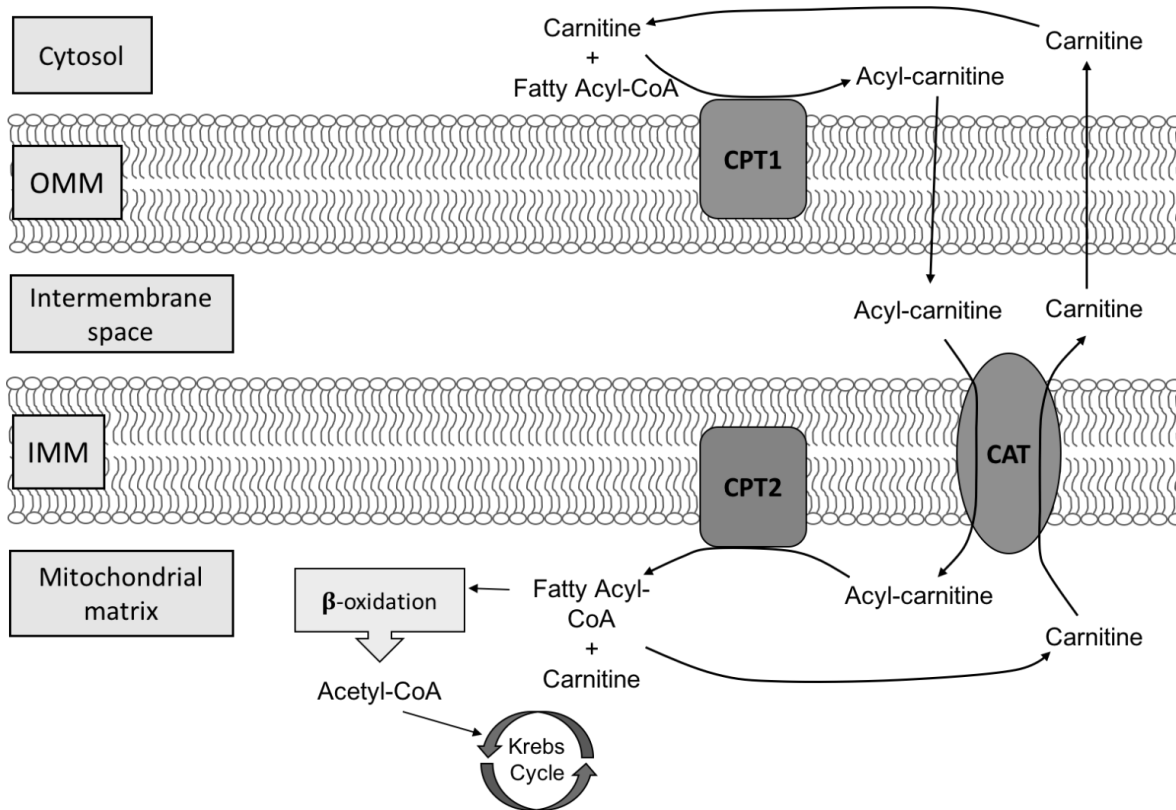
Figure 1.4 Schematic of fatty acyl-CoA transport into the mitochondrial matrix. Fatty acyl-CoAs are converted into acyl-carnitines by carnitine palmitoyltransferase-1 (CPT1). Acyl-carnitine then diffuses across the outer mitochondrial membrane (OMM) into the intermembrane space (IMS) where carnitine-acylcarnitine transferase (CAT) transports it into the mitochondrial matrix. In the matrix, the carnitine is cleaved from the fatty acyl-CoA by carnitine palmitoyltransferase-2 (CPT2). The carnitine is transported into the IMS by CAT, and the fatty acyl-CoA undergoes β-oxidation to produce acetyl-CoA. Acetyl-CoA may enter the Krebs cycle to ultimately produce substrates for the ETS. This diagram represents work from Kerner and Hoppel (2000), McGarry and Brown (1997), and Pande (1975).

transport flavoprotein, NADH, $FADH_2$ and succinate by either ETS complex I or II. Electrons released during substrate oxidation are transported to the increasingly electronegative complexes III and IV. The last redox reaction, catalyzed by complex IV, donates electrons to O_2, the terminal electron acceptor, producing water. The redox reactions at ETS complexes I-IV release free energy, some of which is used to pump protons from the matrix to the IMS, thus generating the PMF. Because O_2 reduction to water represents the final step of the ETS, oxygen "consumption" is typically used as a general measure for total mitochondrial respiration.

In mitochondria from most tissues, the PMF is used as a source of potential energy by ETS complex V (F_1F_O ATPase) to synthesize ATP. However, BAT mitochondria express little F_1F_O ATPase (Cannon, 1977). Moreover sympathetic stimulation of BAT results in the activation of UCP1, a protein unique to eutherian mammals, that dissipates the PMF, though the mechanism underlying this activation remains unknown (Cannon and Nedergaard, 2004). This dissipation stimulates flux through the ETS but substrate oxidation is effectively uncoupled from ATP synthesis, and virtually all of the free energy released is liberated as heat (Fig. 1.5). The futile cycling of protons across the IMM stimulates these reactions and thus the heat release is amplified by the dissipation of the PMF (Staples, 2016).

In the late summer and early autumn, ground squirrels exhibit an increase in the mass of axillary BAT pads accompanied by an increase in the abundance of BAT mitochondria (Ballinger et al., 2016; Milner et al., 1989). These changes are

accompanied by increased expression of several genes involved in BAT

uncoupled thermogenesis, such as those encoding for UCP1 (Ballinger et al.,

2016; Hampton et al., 2013). These changes increase the BAT thermogenic

capacity of hibernators before and throughout the winter.

1.3 Regulation of metabolic suppression in torpor

The thirteen-lined ground squirrel is an excellent model species that has

been used to study the profound and reversible suppression of whole-animal

metabolism seen during entrance into and arousal from torpor. Mitochondrial

metabolism in several tissues of the thirteen-lined ground squirrel has been

studied extensively (Staples, 2016). In skeletal and cardiac muscle mitochondrial

respiration is suppressed by up to 60% in torpor, compared with IBE (Brown and

Staples, 2014). The liver has been shown to have the greatest degree of

mitochondrial metabolic suppression. Liver mitochondrial metabolism is

suppressed by up to 70% in torpor, compared with IBE, (Brown et al., 2012;

Chung et al., 2011; Muleme et al., 2006) but the mechanism behind this

suppression is unknown. Whatever the mechanism may be, it is rapid and

reversible, but it is also temperature sensitive. The suppression of mitochondrial

metabolism is initiated rapidly during entrance into torpor when T_b is high (Chung

et al., 2011), and reversed more slowly during arousal from torpor (Armstrong

and Staples, 2010), when T_b is low. All of these characteristics suggest that the

reversible suppression of mitochondrial metabolism is enzyme-mediated, as
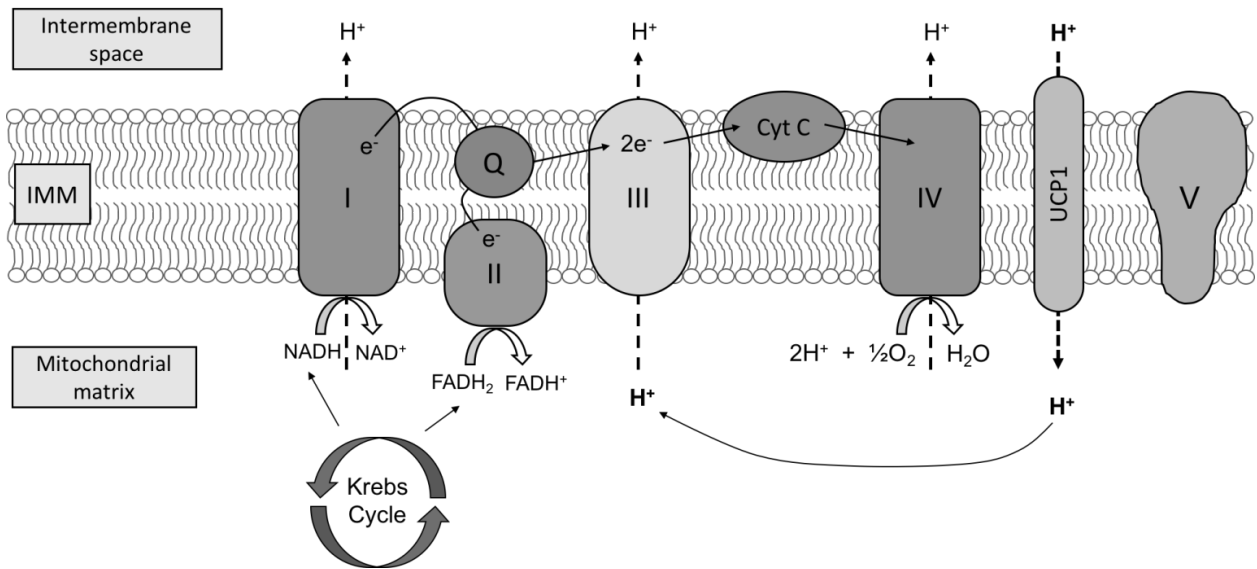
Figure 1.5 Schematic of the BAT mitochondrial electron transport system (ETS). Substrates are oxidized by either complex I or II. Electrons released during substrate oxidation in complexes I and II are transported to increasingly more electronegative complexes III and IV via the Quinone-pool (Q) and ultimately are donated to O_2 by complex IV to produce H_2O. The redox reactions at ETS complexes I, III, and IV release sufficient free energy to pump protons from the matrix to the intermembrane space, thus generating the PMF. Activation of uncoupling protein-1 (UCP1) by acyl-carnitines dissipates the PMF by allowing translocation of protons down the electro-chemical gradient without generating ATP. This futile cycling of protons across the inner mitochondrial membrane (IMM) stimulates the redox reactions catalyzed by the ETS complexes. This is the source of heat for uncoupled thermogenesis.

enzymes can quickly reverse reactions and the rates of these reactions would follow the Q_{10} effect.

Enzyme-mediated post-translational modification of ETS enzyme complexes has been investigated in the thirteen-lined ground squirrel as a potential mechanism behind mitochondrial suppression. Mathers et al. (in press) measured maximal activities of ETS complexes and found that there was significant suppression of the maximal activity of ETS complexes I and II in torpor compared with IBE. These results suggest that the changes in metabolism of intact mitochondria between torpor and IBE depend upon rapid and reversible changes in activities of these enzyme complexes. Such a pattern is consistent with post-translational modification.

1.4 Objectives and Hypothesis

Unlike the liver, mitochondrial metabolism of BAT is regulated by a well-studied adrenergic system; it can be rapidly activated or inhibited in the presence or absence of NE, respectively. Thus, I hypothesize that brown adipose tissue metabolism is solely regulated by the sympathetic nervous system via NE stimulation, with no further functional regulation at the level of the mitochondria or ETS complexes. I predicted that mitochondrial and cellular respiration rates, as well as ETS enzyme activities would not differ between the hibernation states of torpor and IBE.

My first objective was to determine if there was BAT mitochondrial metabolic suppression in torpor, as seen in other tissues such as liver. My second

objective was to investigate the effect of temperature on BAT mitochondrial metabolism in hibernation, as this tissue must sustain function at very low T_b. To investigate a higher level of organization and assess potential regulatory differences in this tissue between these two metabolic states, my third objective was to assess the respiration of intact isolated brown adipocytes and their response to NE stimulation and temperature changes. In order to achieve my objectives, I used high-resolution respirometry and spectrophotometric assays at two biologically relevant temperatures to assess the metabolism of BAT during the hibernation cycle and how temperature affects this process in the thirteen-lined ground squirrel (*Ictidomys tridecemlineatus*).

CHAPTER 2

MATERIALS AND METHODS

2.1 Experimental animals

All experiments were approved by the University of Western Ontario Animal Use Subcommittee (Appendix A) and followed guidelines of the Canadian Council on Animal Care. The thirteen-lined ground squirrels (*Ictidomys tridecemlineatus*) used in this study were either live-trapped in Carman, Manitoba, Canada (49.4° N, 98.0° W) (Brown and Staples, 2014) or bred in captivity at the University of Western Ontario following husbandry guidelines published previously (Vaughan et al., 2006). The squirrels were housed at 25°C ± 3°C and with the same photoperiod as Carman, MB (adjusted weekly) from April until November. In November animals were moved to environmental chambers where the temperature was decreased 1°C /day until it reached 4°C ± 2°C. At this time, photoperiod was reduced to 2 h light (allowing for animal care procedures) and 22 h dark to simulate burrow conditions in the wild. Food and water were provided *ad libitum* until torpor was observed, after which food was withdrawn because this species does not eat throughout the hibernation season.

2.2 Radio telemetry implants

Prior to transfer to the environmental chamber, temperature-sensitive radio telemeters (Model TA-F10, Data Sciences International, Arden Hills MN) were implanted into the peritoneal cavity under isofluorane gas anesthesia (Muleme et al., 2006). Squirrels were provided with postoperative analgesia upon completion

of surgery (subcutaneous injections of Metacam: 1 mg/kg, once per day for 3 days post-surgery)). Core body temperature measurements were collected every four minutes using telemetry receivers (model RA1010, Data Sciences International). Collection of T_b data was performed using Dataquest ART software (Data Sciences International) and used to determine hibernation state in real time.

2.3 Hibernation state

Squirrels in this study were considered either torpid (with a stable T_b near 5°C for at least 3-4 days) or spontaneously aroused into IBE (with a stable T_b near 37°C for 2-4 h). IBE animals were sacrificed with an anesthetic overdose (Euthanyl, 240 mg/mL, 0.2 mL/100 g), which does not affect mitochondrial metabolism (Takaki et al., 1997). Torpid animals were euthanized immediately by cervical dislocation, as handling and an injection of Euthanyl may have forced an arousal. Brown adipose tissue was collected from both left and right axillary regions of each animal. Approximately 2 g of BAT was used for each mitochondrial and adipocyte isolation (see following sections). There was no significant difference (t_{14}= 2.101, P=0.46) in body mass between the animals in the torpor (185.3 g ± 8.7 g S.E.M.) or IBE groups (175.2 g ± 10.3 g S.E.M). Both torpor and IBE groups consisted of 6 females and 2 males. The dates of sampling for each individual can be seen in Figure 2.1.
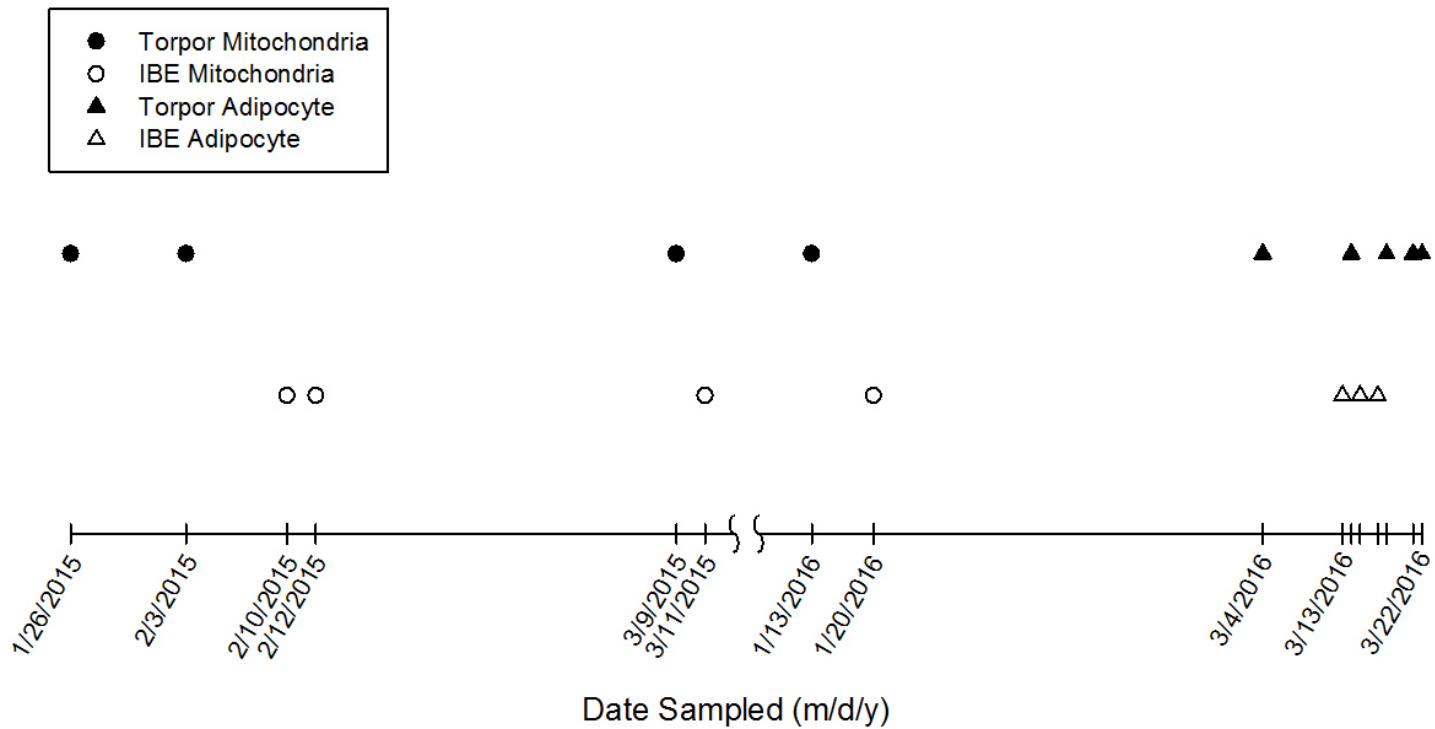
Figure 2.1 Timeline illustrating the date each individual was sampled. Circles represent individuals sampled for mitochondrial respiration experiments. Triangles represent individuals sampled for adipocyte respiration experiments. Black symbols represent individuals that were torpid when sampled. White symbols represent individuals that were in interbout euthermia (IBE) when sampled.

2.4 Isolation of mitochondria

Mitochondria were isolated through differential centrifugation following methods adapted from Cannon and Nedergaard (2008) and Muleme et al. (2006). Brown adipose tissue was initially minced and mechanically homogenized in a glass mortar with a Teflon pestle (4-5 strokes) in homogenization buffer (HB; 250 mM sucrose, 1 mM EGTA, 10 mM HEPES, pH 7.4). The homogenate was then filtered through two layers of cheesecloth and centrifuged for 10 min at 8700 g. The pellet was resuspended in HB and centrifuged for 10 min at 800 g. The supernatant (containing mitochondria) was transferred carefully to a clean tube and the pellet was discarded. The supernatant was centrifuged at 8700 g for 10 min. The resulting mitochondrial pellet was resuspended in HB and centrifuged again at 8700 g for 10 min twice more. The pellet was then re-suspended in 2 mL of HB and kept on ice until use. Isolated mitochondria were used immediately for assessment of mitochondrial respiration (see section 2.5), and aliquots were frozen at -80°C for subsequent enzyme assays. Total mitochondrial protein content was quantified by Bradford assay (Bradford, 1976). A 5 μL aliquot of mitochondrial sample was diluted in 95 μL of HB and 10 μL of this diluted sample was added to 200 μL of Bradford assay solution (1:4 double distilled H_2O: Bradford protein assay solution; Bio-Rad, Mississauga ON) in triplicate and mixed. Upon completion of the reaction (30 min), the absorbance (595 nm) was measured using a spectrophotometer (SpectraMax 340PC, Molecular Devices, Toronto ON). Standards consisted of bovine serum albumin (BSA) dissolved in HB.

2.5 Mitochondrial respiration

Respiration rates of isolated BAT mitochondria were evaluated with high-resolution respirometry using Clark-type polarographic oxygen electrodes (Oxygraph-2k; Oroboros, Innsbruck AT) in 2 mL of respiration buffer (110 mM sucrose, 60 mM K-lactobionate, 20 mM HEPES, 20 mM taurine, 10 mM KH_2PO_4, 3 mM $MgCl_2$, 0.5 mM EGTA, pH 7.1, 1% (w/v) fatty-acid free BSA). The Oxygraph-2k was calibrated with air-saturated buffer, as well as oxygen-depleted buffer (obtained with a yeast suspension). All measurements were performed with constant stirring (750 rpm) and constant temperature, either 10°C or 37°C for each individual animal. These two temperatures were chosen to simulate T_b during torpor and IBE, respectively. Although the T_b of these squirrels in torpor is ~5°C, the Oxygraph-2k only produced consistent results at temperatures of 10°C or higher. All substrates were dissolved in respiration buffer (except oligomycin which was dissolved in ethanol) and final concentrations reported represent those in the 2 mL Oxygraph-2k chamber.

Respiration rates were determined with pyruvate (1 mM) and octanoyl carnitine (2.5 mM both with 1mM malate) as oxidative substrates, and were standardized to mitochondrial protein content. To confirm that these respiration rates were UCP1 mediated, guanosine 5'-diphosphate (GDP; 1 mM) was added to inhibit the flux of protons through UCP1 (Cannon and Nedergaard, 2008). Adenosine 5'-diphosphate (ADP; 1 mM) was then added to assess "coupled" Complex V mediated respiration rates (i.e. "state 3"), which were then inhibited by oligomycin (1.25 μM). An example is depicted in Figure 2.2, which shows that
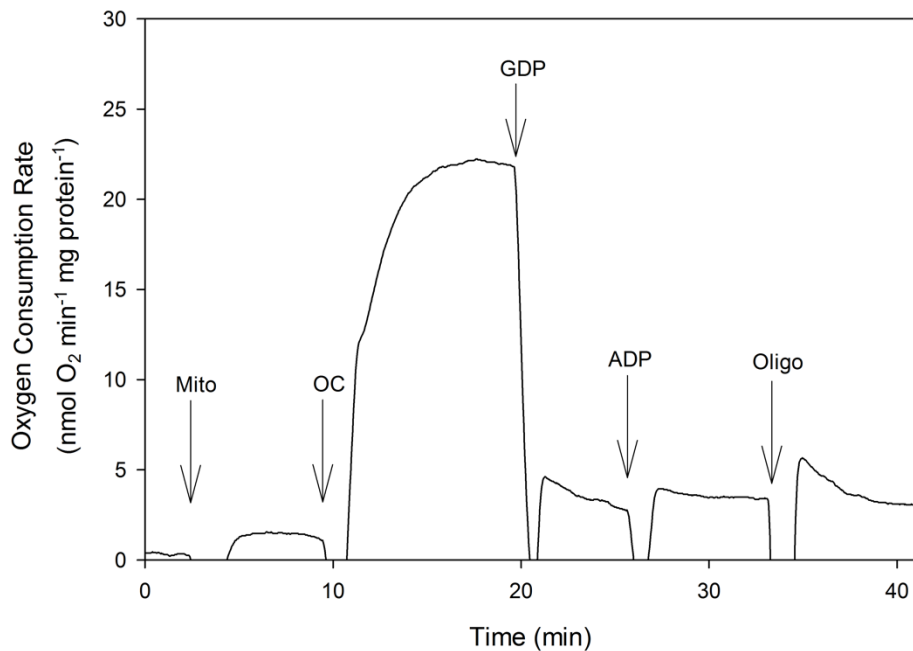
Figure 2.2 Oxygen consumption of isolated brown adipose tissue mitochondria from one IBE animal measured at 10°C using octanoyl carnitine as a fuel. Arrows indicate times at which the following additions were made: Mito, isolated mitochondria (0.23 mg protein); OC, octanoyl carnitine and malate (2.5 mM and 1 mM, respectively); GDP, guanosine 5'diphosphate (1 mM); ADP, adenosine 5'-diphosphate (1 mM); Oligo, oligomycin (1.25 μM).

the addition of octanoyl carnitine (OC), with malate, produced a high state 2 (uncoupled) respiration rate. Most of the state 2 rate was UCP1 mediated, as the addition of GDP caused a decrease in oxygen consumption. Adding ADP supported only low coupled (state 3) rates, which is consistent with very low concentrations of Complex V in BAT mitochondria compared to the other ETS enzymes. The addition of oligomycin (Oligo) inhibited ETS Complex V, so its addition had little effect on the state 3 respiration rate (Cannon and Nedergaard, 2008).

2.6 Enzyme assays

To investigate mechanisms underlying any differences seen in the mitochondrial respiration experiments, I conducted spectrophotometric enzyme assays. If the results of these assays mirrored those of the respiration experiments, these mechanisms would likely involve direct alterations of the ETS enzymes themselves, similar to those seen in liver mitochondria (Mathers et al., in press). Mitochondrial ETS enzyme assays were adapted from methods outlined by Kirby et al., (2007). Frozen isolated mitochondrial aliquots were thawed and centrifuged at 20,000 g and 4°C for 10 min. These pellets were resuspended in hypotonic medium (25 mM K_2HPO_4, 5 mM $MgCl_2$, pH 7.4) containing phosphatase and deacetylase inhibitors (1% Phosphatase Inhibitor Cocktail 3, Sigma-Aldrich; 1% Deacetylation Inhibition Cocktail, Santa Cruz Biotechnology) to a concentration of 1 mg protein/mL and frozen and thawed three times using liquid nitrogen and cold water.

All assays that were performed at 37°C used a SpectraMax 340PC plate spectrophotometer (Molecular Devices, Toronto ON) and were conducted in 96-well polystyrene microplates rather than individual cuvettes. Assay conditions were adapted accordingly for triplicate assays in 350 μL wells. All assays performed at 10°C used a Cary 100 UV/Vis spectrophotometer (Varian, Palo Alto, CA) with disposable polystyrene cuvettes and a 1 mL reaction volume. Temperature was maintained using a Peltier temperature control module. Base-line readings were taken before each reaction was started and reaction conditions are outlined in Table 2.1.

2.7 Isolation of brown adipocytes

To investigate whether any changes noted in mitochondria translate to a higher level of organization, I compared oxygen consumption rates of brown adipocytes isolated from ground squirrels in torpor and IBE. Brown adipocytes were isolated following methods adapted from Cannon and Nedergaard (2008). The axillary BAT of one squirrel was dissected out and placed in a small volume of ice-cold Krebs/Ringer phosphate buffer (109 mM NaCl, 6.9 mM KCl, 1.5 mM CaCl$_2$, 1.4 mM MgSO$_4$, 16.7 mM Na$_2$HPO$_4$, 5.6 mM NaH$_2$PO$_4$, 20 mM glucose, 4% fatty-acid-free bovine serum albumin, pH 7.4) and carefully cleaned of contaminating tissues. The tissue was then weighed and placed in a 50 mL polyethylene conical tube containing 5 mL Krebs/Ringer phosphate buffer with 1.66 mg/mL collagenase (Collagenase Type II, Worthington Biochemical). The tissue was pre-incubated for 5 mins in a slowly shaking water bath at 37°C after

24

which an additional 5 mL of buffer was added. The conical tube was then vortexed for 5 seconds. The tissue was filtered onto 250 μm nylon mesh and the first filtrate was discarded. The tissue was collected from the mesh using forceps and placed into a small volume (~1 mL) of buffer on a square of Parafilm. The tissue was minced with scissors and then added back to a 50 mL conical tube with 5 mL of Krebs/Ringer phosphate buffer with collagenase. The conical tube containing the tissue mince was incubated for 25 mins in the shaking water bath at 37°C with 5 seconds of vortexing every five mins. The conical tube was then removed from the water bath, 5 mL of buffer with collagenase was added and the tube was vortexed for 15 seconds. The contents of the tube were filtered through 250 μm nylon mesh and the filtrate was collected into a 50 mL centrifuge tube and placed upright on ice to settle. The tissue pieces remaining on the mesh were collected with forceps and placed back into the 50 mL conical tube with 5 mL buffer with collagenase and incubated in the shaking water bath for 15 mins. The conical tube was removed from the water bath, 5 mL of buffer with collagenase was added and the tube was vortexed for 15 seconds. The contents of the tube were filtered through 250 μm nylon mesh and the filtrate was collected into the same 50 mL centrifuge tube on ice and was left to settle. The remaining tissue pieces were collected again and re-incubated as above to increase yield. The 50 mL centrifuge tube containing all of the above filtrates was then centrifuged at 60 *g* for 5 mins, covered with Parafilm and left to stand and settle for at least 30 mins on ice.

Table 2.1 ETS enzyme assay reaction conditions for both 37°C and 10°C.

Enzyme	Assay Temperature	Mitochondrial Sample (μg of total protein)	Reaction Conditions	Baseline reading before addition	Absorbance Wavelength
Complex I	37	10	25 mM K_2HPO_4 (pH 7.2) 2 μg/mL antimycin A 2 mM KCN	mitochondrial sample	340 nm
	10	50	2.5 mg/mL BSA 0.2 mM NADH		
Complex II	37	5	25 mM K_2HPO_4 (pH 7.2) 2 μg/mL rotenone 2 μg/mL antimycin A 2 mM KCN	ubiquinone$_1$	600 nm
	10	50	20 mM succinate 50 μM dichlorophenolindophenol 0.1 mM ubiquinone$_1$		
Complex III	37	1	25 mM K_2HPO_4 (pH 7.2) 2 μg/mL rotenone 2 mM KCN 2.5 mg/mL BSA	ubiquinone$_2$	550 nm
	10	10	0.6 mM n-dodecyl-β-D-maltoside 15 mM oxidized cytochrome c 0.26 mM ubiquinone$_2$		
Complex IV	37	1	25 mM K_2HPO_4 (pH 7.2) 5 mM $MgCl_2$ 2.5 mg/mL BSA	mitochondrial sample	550 nm
	10	5	0.6 mM lauryl maltoside 50 μM reduced cytochrome c		
Complex V	37	3	5 mM ATP 1 mM phosphoenolpyruvate 0.2 mM NADH	mitochondrial sample	340 nm
	10	40	1 U/mL pyruvate kinase 1 U/mL lactate dehydrogenase		

Cells were carefully collected from the adipocyte layer using a Pasteur

pipette and bulb. The cells were localized to a small layer very near the surface of

the supernatant, immediately below the fat layer that accumulated on the surface.

The isolated cells were kept on ice for the remainder of the day, approximately 4

hours. Cells were counted on a hemocytometer. Viability was determined using

trypan blue; 0.5 mL of 0.4% Trypan Blue solution (w/v in water, 0.81% NaCl,

0.06% K_2HPO_4; Sigma Aldrich) was added to a glass vial with 0.2 mL of cell

suspension and 0.3 mL of Krebs/Ringer phosphate buffer and allowed to stand at

room temperature for 10 mins. Cells were counted using a hemocytometer at 100x

magnification with a light microscope to calculate the cell viability; viable cells

remained a beige colour while dead cells allowed the Trypan Blue to enter and

appeared blue. All cell suspensions had >95% viability. Positive controls for this

cell viability assay were conducted with a small volume of cell suspension that

was heated to 75°C for 2 minutes. All positive controls had 100% inviability

based on Trypan Blue staining. Following all respiration measurements,

remaining cells were aliquoted and frozen at -80°C.

2.8 Adipocyte respiration

Respiration rates of isolated brown adipocytes were evaluated with high-

resolution respirometry using the Oxygraph-2k in 2 mL of Krebs/Ringer

bicarbonate buffer (118 mM NaCl, 6 mM KCl, 2.5 mM $CaCl_2$, 1.2 mM $MgSO_4$,

1.2 mM NaH_2PO_4, 25.3 mM $NaHCO_3$, 20 mM glucose, 4% fatty-acid-free BSA,

pH 7.4, equilibrated with 5% CO_2 in air). The Oxygraph-2k was calibrated to air-

saturated and oxygen-depleted (obtained with a yeast suspension) buffer. All measurements were performed with constant stirring (750 rpm) and constant temperature, either 10°C or 37°C. Cells were added to Oxygraph-2k chamber to a final concentration of 80 000 cells/mL buffer and a basal respiration rate was recorded. The light in the chamber was turned off, as norepinephrine (NE, L-(-)Norepinephrine(+)-bitartrate salt monohydrate) is light sensitive, and NE was added to a final concentration of 1 mM to achieve the NE stimulated rate. An example trace is shown in Figure 2.3.

2.9 Statistical analyses

All values are represented as mean ± S.E.M. unless otherwise stated. All statistical analyses were conducted using R software (R Core Team 2015). Statistical significance was determined by Student's t-tests for two-group comparisons (two-tailed; body mass and ETS enzyme assays, one-tailed; Q_{10} values). Split-plot ANOVAs with Fisher's LSD post-hoc analyses were used to assess significant differences between hibernation state and temperature for mitochondrial (both fuels) and cellular respiration rates (basal and NE stimulated rates and the fold change between basal and stimulated rates). Statistical differences were considered significant when $P < 0.05$.
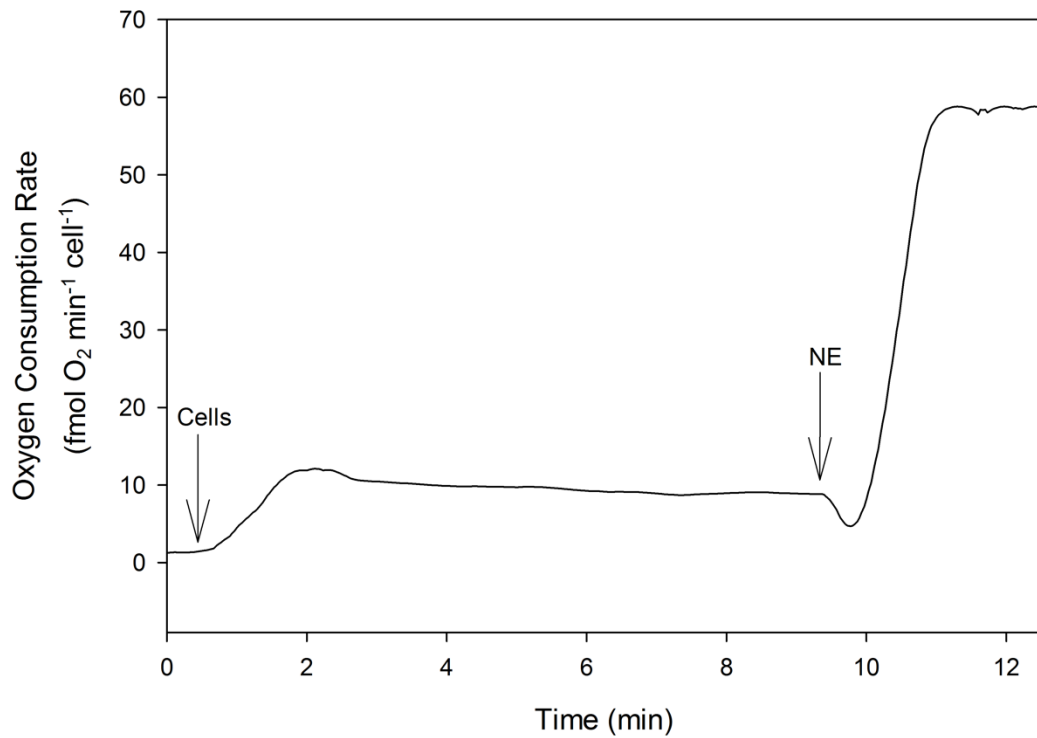
Figure 2.3 Oxygen consumption of isolated brown adipose tissue adipocytes from one IBE animal measured at 10°C. Arrows indicated times at which the following additions were made: cells (80 000 cells/mL) were added and a basal respiration rate was recorded; norepinephrine (NE, 1 mM) was added to achieve the NE stimulated rate

CHAPTER 3

RESULTS

3.1 Mitochondrial respiration

When assayed *in vitro* at 37°C, BAT mitochondria isolated from IBE animals displayed 62% higher respiration rates than those isolated from torpid animals, regardless of whether the oxidative substrate was pyruvate (Fig. 3.1A; $F_{1,6}$=11.344, P=0.015) or octanoyl carnitine (Fig. 3.1B; $F_{1,6}$=9.659, P=0.021). When measured at 10°C there was an opposite trend, with respiration rates from torpid animals appearing to be higher than IBE (pyruvate: 48% and octanoyl carnitine: 38%), though the differences were not statistically significant (Fig. 3.1A; $F_{1,6}$=6.031, P=0.057 and Fig.3.1B; $F_{1,6}$=4.614, P=0.075).

3.2 Enzyme assays

To assess a potential mechanism underlying suppression of BAT mitochondrial metabolism in torpor I compared maximal activities of the five ETS enzyme complexes using homogenized, isolated mitochondria from IBE and torpid animals. There were no significant differences in maximal enzyme activity between IBE and torpor for any of the five ETS complexes, regardless of whether assays were performed at 10°C (Fig 3.2A: Complex I t_6=-0.250, P=0.838; Complex II t_6=0.945, P=0.486; Complex III t_6=-0.429, P=0.702; Complex IV t_6=-0.245, P=0.371; Complex V t_6=-0.205, P=0.847) or 37°C (Fig. 3.2B:, Complex I t_{14}=2.201, P=0.521; Complex II t_{14}=2.179, P=0.482; Complex III t_{14}=2.201, P=0.743; Complex IV t_5=12.706, P=0.402; Complex V t_{14}=2.145, P=0.266).
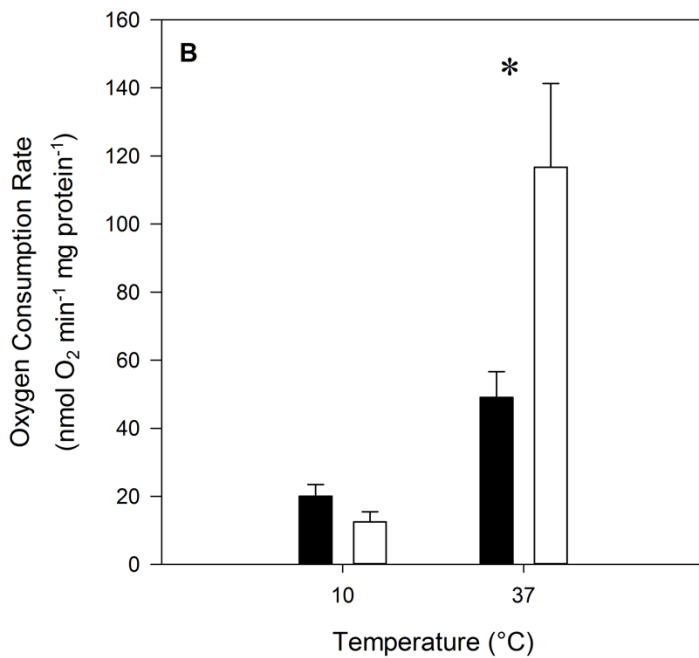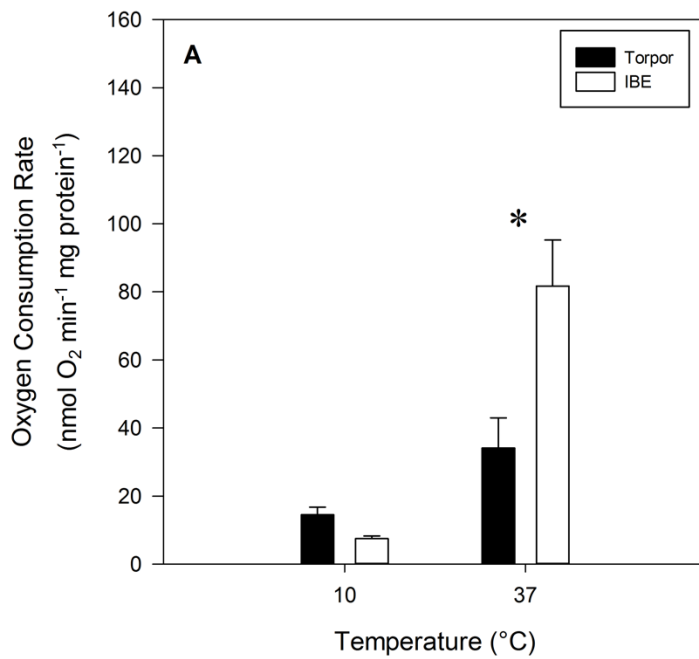
Figure 3.1 Mitochondrial state 2 oxygen consumption rates from isolated brown adipose tissue mitochondria using (A) pyruvate and (B) octanoyl carnitine as oxidative substrate. Respiration rates of isolated mitochondria were standardized to protein concentration. Values represent mean + S.E.M. and n=4 for all groups. Statistical significance between torpor and IBE is denoted with an asterisk ($P<0.05$).
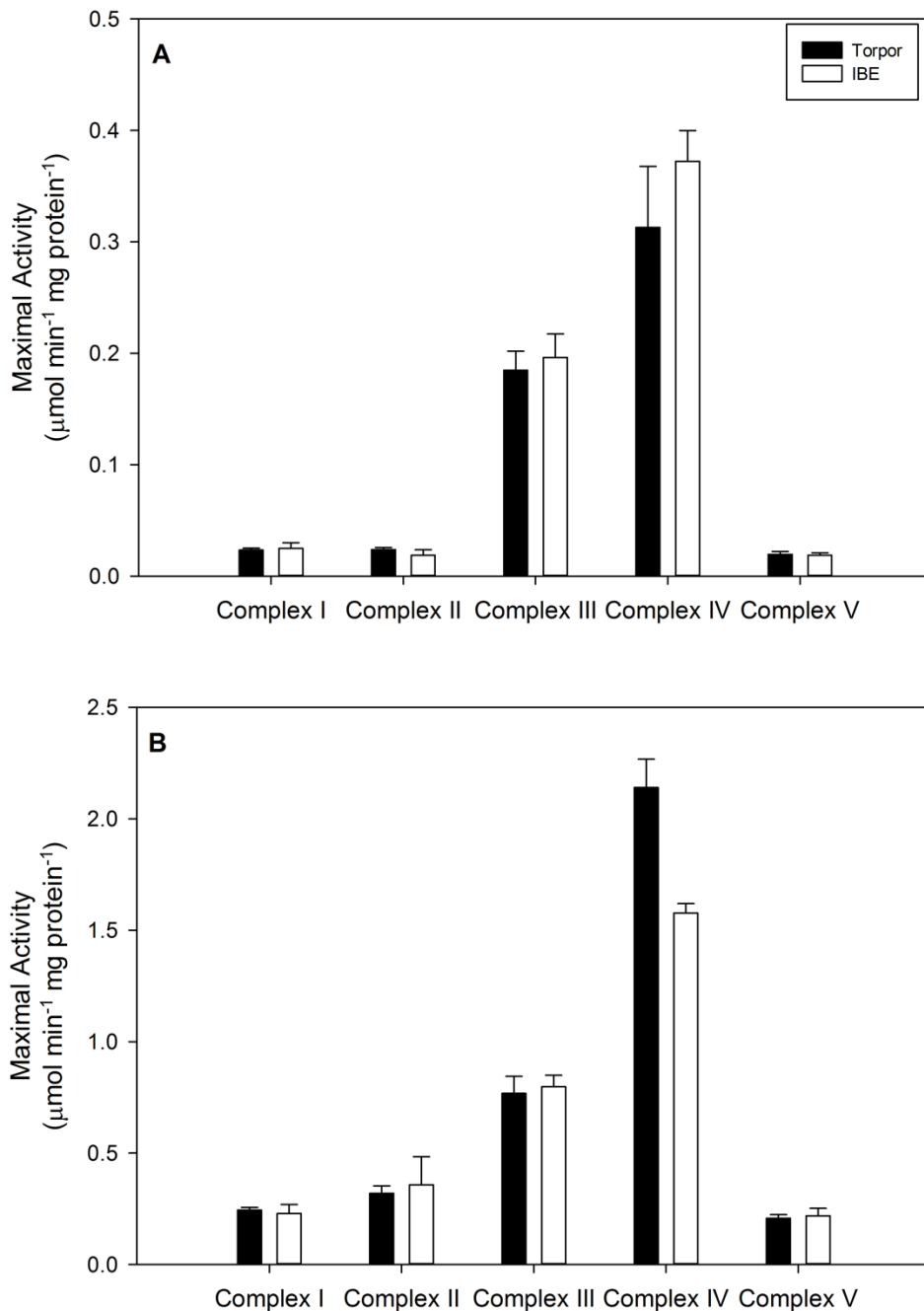
Figure 3.2 Maximal enzyme activity of electron transport system complexes using homogenized, isolated, brown adipose tissue mitochondria assayed at (A) 10°C and (B) 37°C and standardized to protein content. Values are mean + S.E.M, except where sample size < 3 in which case error bars represent range. Sample sizes for 10°C activities are 6 (Torpor) and 2 (IBE) for all five complexes. Sample sizes for 37°C activities are 9 (Torpor) and 7 (IBE) for complexes I, II, III, and V. Sample sizes for Complex IV 37°C rates are 5 (Torpor) and 2 (IBE). No significant differences were observed between hibernation states for any of the complexes (P>0.05).

3.3 Temperature effects and Q_{10}

To further examine the effects of temperature on mitochondrial metabolism, I plotted respiration rates for mitochondria isolated from the same individuals at both experimental temperatures (Fig. 3.3). While there is some overlap between IBE and torpor at 10°C, there is clear separation at 37°C, with all of the IBE individuals having higher rates. From these data I calculated Q_{10} values for each individual. The mean Q_{10} values of uncoupled respiration in mitochondria isolated from torpid animals were significantly lower than those isolated during IBE, regardless of substrate (Table 3.1; pyruvate t_6=5.727, P=0.002 and octanoyl carnitine t_6=5.275, P=0.002). In contrast to the intact mitochondria, the Q_{10} values from the maximal activities of ETS enzymes ranged from 1.68 to 2.97 and were quite similar between torpor and IBE for each ETS complex (Table 3.2). These values were calculated from the mean maximal activities of each ETS complex for both temperatures, as Q_{10} values could not be calculated for each individual at each temperature due to low sample sizes in some groups.
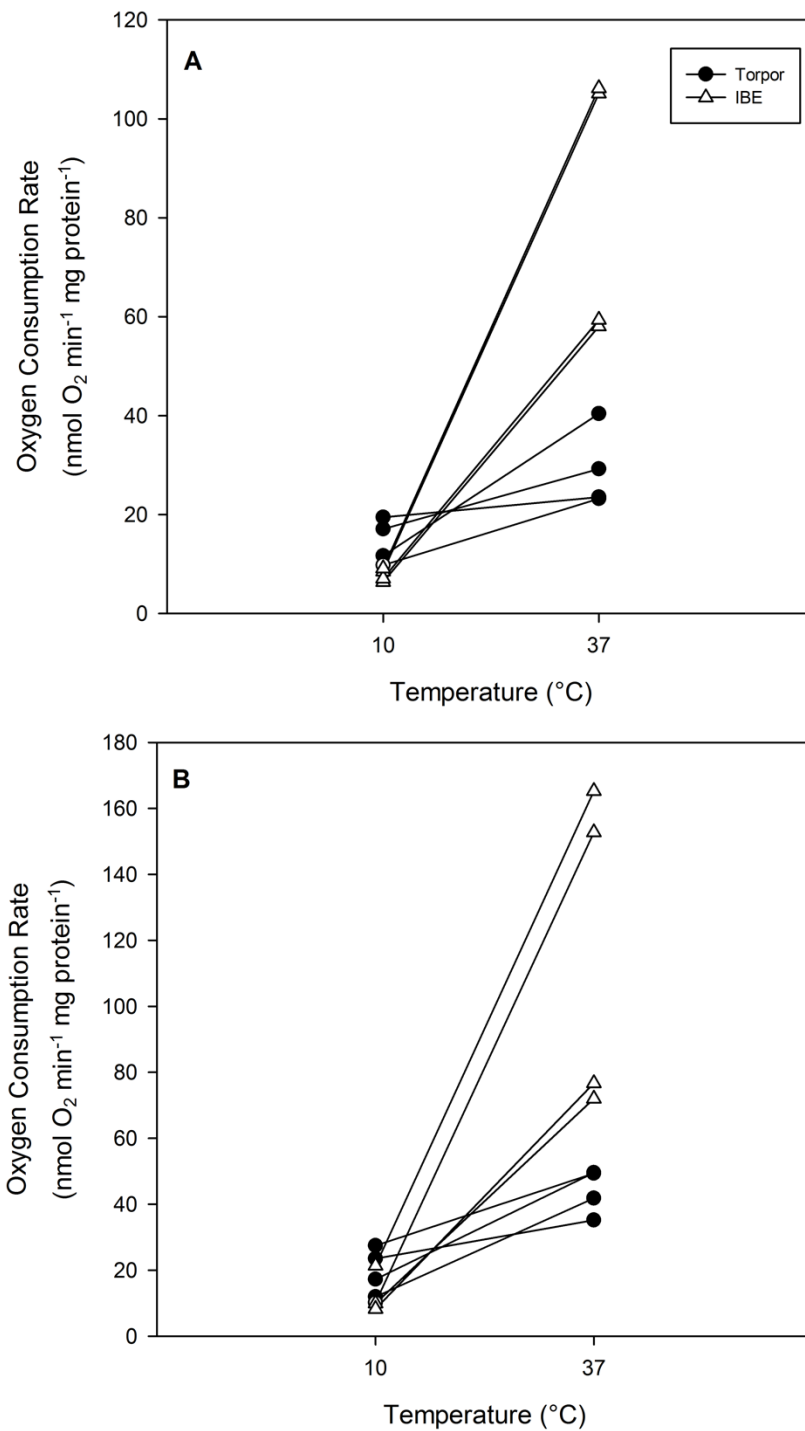
Figure 3.3 Interaction plots of mitochondrial oxygen consumption rates from isolated brown adipose tissue mitochondria assayed *in vitro* at 10°C and 37°C using (A) pyruvate and (B) octanoyl carnitine as oxidative substrate. Points connected by a line represent data from the same individual, summary data is found in Fig. 3.1. This plot illustrates the relationship between measurements from the same individual to emphasize temperature-sensitivity trends.

Table 3.1 Mean Q_{10} values for mitochondrial respiration rates at 10°C and 37°C.

Oxidative substrate	Q_{10}	
	IBE	Torpor
pyruvate	2.40 ± 0.06	1.38 ± 0.17*
octanoyl carnitine	2.30 ± 0.15	1.42 ± 0.13*

Values are derived from mitochondrial respiration rates measured from each individual at each temperature, plotted in Fig. 3.3. Asterisks represent significant difference from IBE value and P=0.002 for both substrates.

Table 3.2 Q_{10} values for maximal ETS enzyme activities calculated from mean maximal enzyme activities at 10°C and 37°C.

Enzyme	Q_{10}	
	IBE	Torpor
Complex I	2.27	2.38
Complex II	2.61	2.97
Complex III	1.69	1.68
Complex IV	1.71	2.04
Complex V	2.47	2.40

Values were calculated from the mean maximal activities of each ETS complex, as small sample sizes in some groups did not allow for individual calculations.

3.4 Adipocyte respiration

Basal and NE stimulated adipocyte respiration rates did not differ significantly between torpor and IBE at either *in vitro* temperature (Fig. 3.4: Basal $F_{1,7}=0.939$, P=0.365 and NE stimulated $F_{1,7}=1.563$, P=0.251). The Q_{10} values for these respiration rates were all between 2-3 (Table 3.3), which suggests that the temperature sensitivity of BAT adipocyte respiration does not differ between torpor and IBE. To assess any potential differences in NE sensitivity and ability to stimulate respiration rates, I calculated the fold change in respiration rate from basal to NE stimulated rates for each individual and at both temperatures. There were no significant differences in the response of adipocyte respiration to NE between torpor and IBE regardless of *in vitro* assay temperature, with respiration increasing at least 3.6-fold following NE treatment (Fig. 3.5: $F_{1,7}=0.186$, P=0.680).
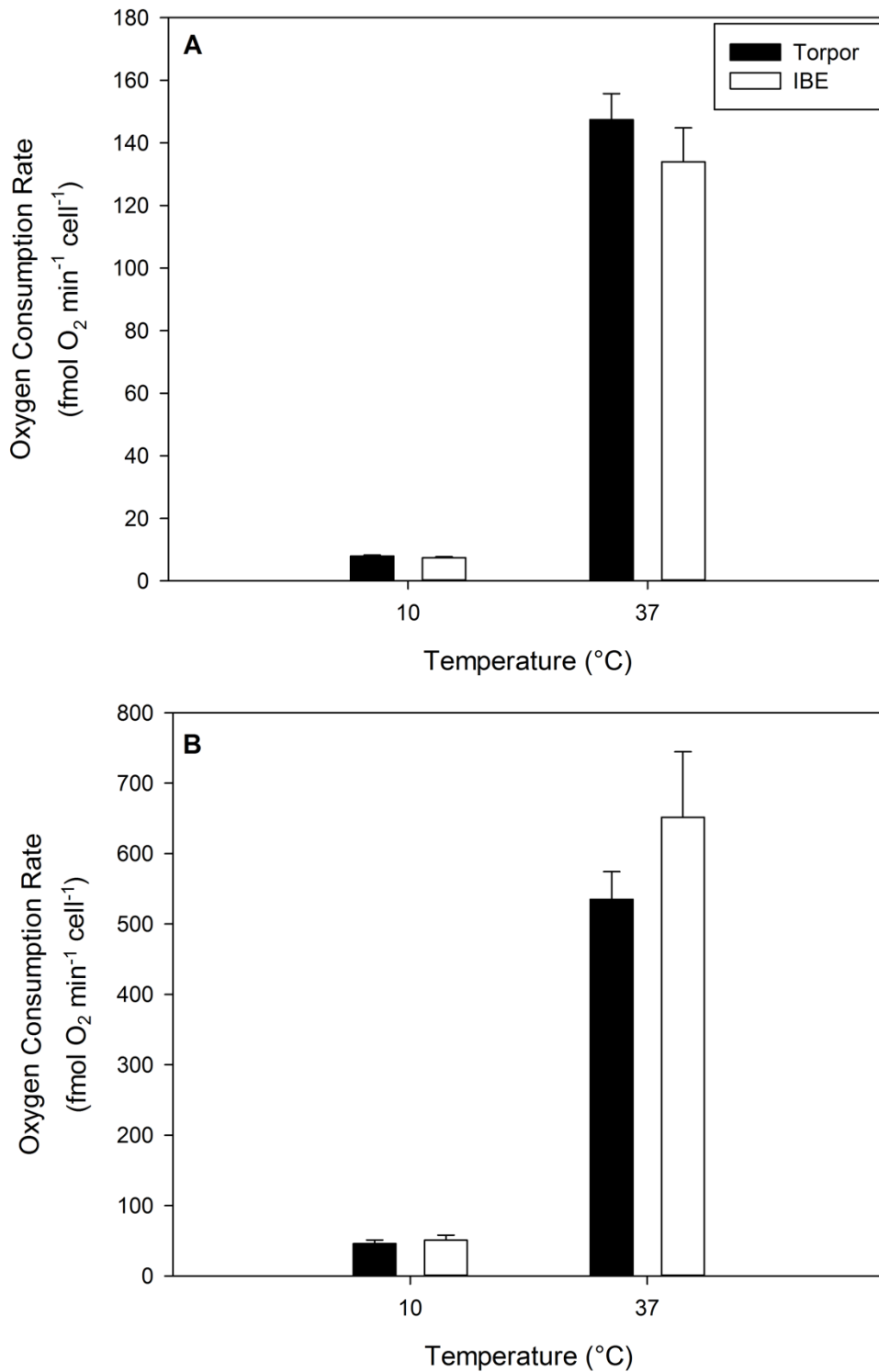
Figure 3.4 Basal (A) and norepinephrine (NE) stimulated (B) oxygen consumption rates of isolated brown adipocytes. Rates are standardized to cell concentration. Values represent mean + S.E.M. There were no significant differences between torpor (n=5) and IBE (n=4).

Table 3.3 Mean Q_{10} values for adipocyte respiration rates at 10°C and 37°C.

Adipocyte respiration rate	Q_{10}	
	IBE	Torpor
basal	2.91 ± 0.06	2.95 ± 0.09
NE stimulated	2.57 ± 0.05	2.50 ± 0.24

Values are derived from adipocyte respiration rates measured from each individual at each temperature Mean adipocyte respiration rates for all groups are plotted in Fig. 3.4 A and B.
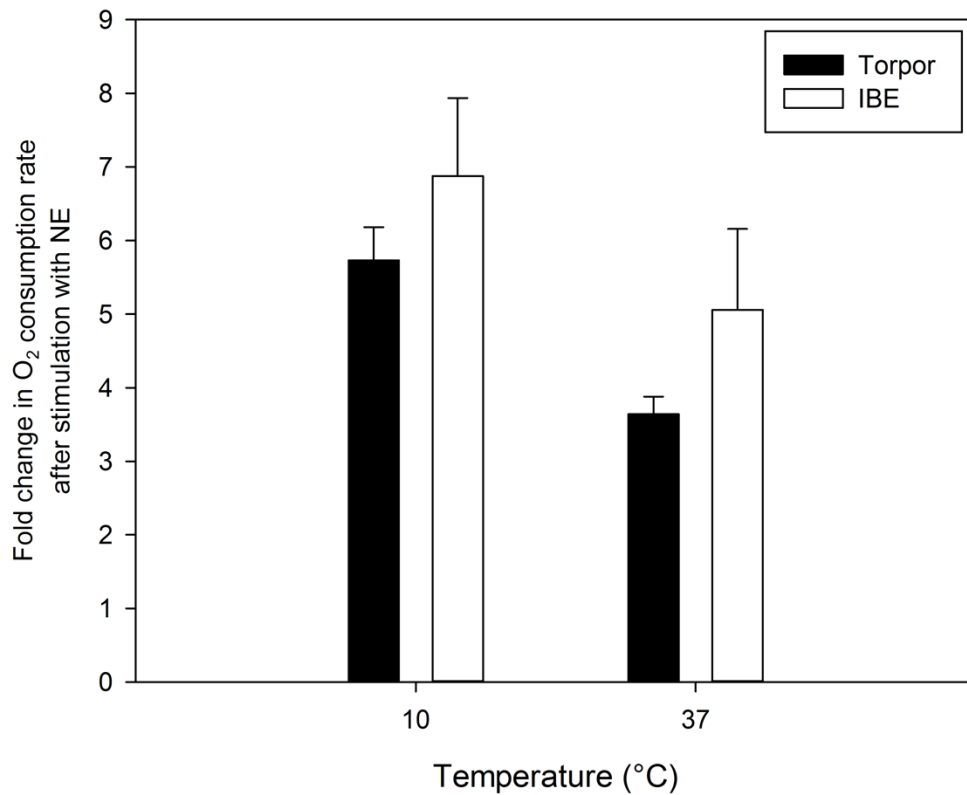
Figure 3.5 Response of oxygen consumption rate to norepinephrine (NE) stimulation in isolated brown adipocytes. The fold change in respiration rate from the basal rate to the NE stimulated rate was calculated for each individual. Values represent mean + S.E.M. There were no significant differences between torpor (n=5) and IBE (n=4).

CHAPTER 4

DISCUSSION

4.1 Mitochondrial respiration and maximal ETS enzyme activities among hibernation states

One goal of this study was to determine if brown adipose tissue mitochondria showed reversible metabolic suppression between hibernation states. In several tissues of hibernators, including liver, skeletal muscle and cardiac muscle, the transition from IBE to torpor corresponds with a significant suppression of mitochondrial respiration (Barger et al., 2003; Brown et al., 2012; Brustovetsky et al., 1989). I hypothesized that there would be no suppression of mitochondrial respiration rates or ETS complex activity between torpor and IBE, because the metabolism of BAT adipocytes and mitochondria is effectively regulated by sympathetic activation. During entrance into torpor, as T_{set} decreases, sympathetic activation of BAT would cease and BAT mitochondrial respiration would fall to a minimum. As a result, further acute suppression of BAT mitochondrial respiration would appear to offer little advantage.

To test this hypothesis, I measured oxygen consumption rates of isolated mitochondria. These rates are in close agreement with those reported in the literature for BAT mitochondria isolated from rats and mice (Cannon and Nedergaard, 2008; Shabalina et al., 2014). Contrary to my predictions, I saw significant suppression in the mitochondrial respiration rates for both fuels at 37°C (Fig. 3.1). This pattern is similar to that observed in liver mitochondria isolated from thirteen-lined ground squirrels; when measured *in vitro* at 37°C,

respiration rates from torpid individuals were significantly suppressed by 70%

when compared with individuals sampled in IBE (Brown et al., 2012). The pattern

reported for liver mitochondria differs from my experiments, however, because

liver mitochondrial respiration in torpor showed no differences when compared

with IBE at 10°C (Brown et al., 2012) while my BAT respiration rates at 10°C

showed a different trend; the BAT mitochondrial respiration rates in my

experiments were 38% and 48% higher with pyruvate and octanoyl carnitine,

respectively, as oxidative substrates in torpor relative to IBE. A very recent study

found no significant differences in BAT mitochondrial respiration rates (state 3

with succinate) between torpor and IBE, apparently contradicting my results in

BAT (Ballinger et al., 2016). In that study, however, the methods used may not

have been entirely appropriate for this tissue, as they used succinate as the

oxidative substrate but BAT oxidizes primarily fatty-acids for uncoupled

thermogenesis (Cannon and Nedergaard, 2008; Nedergaard and Cannon, 1984).

The respiration rates reported by Ballinger et al. (2016), though measured at 25°C

are close to the uncoupled rates I measured at 37°C. Unfortunately Ballinger et al.

(2016) incubated their mitochondria with ADP, but without GDP, so it is

impossible to determine what proportions of these rates can be attributed to

coupled (i.e. complex V-mediated) *vs*. uncoupled (i.e. UCP1-mediated)

respiration. The coupled, state 3 respiration rates that I measured were very low

and often could not be distinguished from the GDP inhibited rates (e.g. Fig. 2.1),

so the significance of the "state 3" data from Ballinger et al. (2016) remains in

question. I believe that the methods that I employed are more relevant to this

tissue as they assess UCP1-mediated respiration using relevant oxidative substrates as a proxy for determining differences in uncoupled thermogenesis in BAT between hibernation states.

I also measured the maximal activity of each ETS complex. As predicted, I found no differences in the activities of ETS complexes between IBE and torpor at either temperature (Fig. 3.2). In liver, however, the activities of some liver ETS enzymes, such as NAHD dehydrogenase (complex I) and succinate dehydrogenase (complex II), from torpid individuals also have lower maximal activities compared with interbout euthermic individuals (Armstrong and Staples, 2010; Mathers et al., in press) even though the amount of these enzymes (as determined by immunoblot) does not change between torpor and IBE (Mathers et al., in press). This reduction in enzyme activity in torpor for liver mitochondria may be due to post-translational modifications of ETS enzymes (Chung et al., 2013; K.E. Mathers and J.F. Staples, unpublished observations). In liver mitochondria, the acute metabolic suppression may also be affected by the remodeling of mitochondrial membrane phospholipids known to occur during arousal (Armstrong et al., 2011).

In my experiments, I found no changes in ETS enzyme activities, so it is unlikely that these enzymes in BAT experience differential post-translational modifications between torpor and IBE as observed in liver. The differences seen in my mitochondrial respiration rates are more likely due to mechanisms that involve changes to the whole, intact organelle, such as membrane remodeling (Else and Wu, 1999). Comparing my results from BAT with those from liver I

conclude that there is likely more than one way to suppress mitochondrial metabolism between torpor and IBE within a single species. The mechanisms of suppression in liver mitochondria seem to be different than those in BAT mitochondria isolated from the same individuals, a novel finding.

4.2 Mitochondrial temperature sensitivity differences among hibernation states

Oxygen consumption rates of BAT mitochondria isolated from torpid animals were suppressed compared with rates from individuals in IBE when measured at 37°C. At 10°C, however, these rates did not differ between torpor and IBE although rates from torpor animals tended to be higher than IBE. These patterns led me to conclude that there is some level of functional regulation at the level of mitochondria that differs between IBE and torpor. For IBE animals, Q_{10} values of mitochondrial respiration rates were typical of most enzyme catalyzed reactions, between 2 and 3 (Fig. 3.3, Table 3.1). In contrast, the respiration rates from torpid animals were comparatively insensitive to temperature with Q_{10} values of ~1.4 (Fig. 3.3, Table 3.1). Liver mitochondrial respiration rates from the same species showed greater Q_{10} values for an assay temperature range of 5°C and 37°C and also showed that there were significant differences in the Q_{10} values between torpor and IBE (Muleme et al., 2006). However, unlike my results, the Q_{10} values for liver mitochondrial respiration (state 3 with succinate) of torpid individuals were >2 suggesting that liver mitochondrial respiration is still sensitive to temperature in torpor (Brown et al., 2012; Muleme et al., 2006).

Substantial temperature changes, such as those experienced during a torpor-arousal cycle, can alter the rates of enzyme-catalyzed reactions and can also alter other enzyme properties, including substrate affinities and subunit associations; these properties are determined by weak bond interactions which are temperature sensitive (Hochachka and Somero, 2002). For membrane-bound enzymes, such temperature effects can be mitigated or amplified by interactions with closely associated membrane components, including phospholipids.

Regulatory mechanisms that involve membrane fluidity and composition are essential in tissues that must function at low temperatures (Heller, 1986; Pehowich et al., 1988), for example during torpor when T_b is ~5°C. The differential temperature sensitivity of BAT mitochondrial respiration exhibited in my experiment leads me to conclude that the mechanism of regulation between IBE and torpor is not directly at the enzyme level but likely involves the intact organelle, since the patterns seen in mitochondrial respiration were not mirrored by the spectrophotometric ETS enzyme assays. In rats (*Rattus norvegicus*) and cane toads (*Bufo marinus*), membrane composition differences have been shown to affect the activity of the Na^+/K^+ ATPase, such that enzymes isolated from toads showed similar activities to rat enzymes when measured in the same membrane compositions (Else and Wu, 1999). This example illustrates the great influence that membrane composition can have on membrane-bound enzyme activities.

The brown adipocyte respiration results also contradicted the mitochondrial respiration results. A similar pattern was observed in liver metabolism studies on golden-mantled ground squirrels (*Callospermophilus*

lateralis), where the metabolic suppression during torpor known to occur in isolated liver mitochondria was not observed in isolated hepatocytes (Staples and Hochachka, 1997). The adipocyte isolation process called for long incubations at high (37°C) temperatures, which likely reversed any changes in enzymes involved in the mechanism of metabolic suppression that I noticed in the isolated mitochondria results. I hypothesize that these mechanisms involve mitochondrial membrane remodeling, as it is an enzyme-mediated process that can account for the rapid and reversible nature of these differences. In hibernating Syrian hamsters (*Mesocricetus auratus*), remodeling of the membrane of the sarcoplasmic reticulum in the heart, specifically an increase in the proportion of linoleic acid (LA) in torpor compared with IBE, significantly increased the activity of sarcoplasmic reticulum $Ca^{2+}-$ATPase 2a (SERCA)(Giroud et al., 2013). These authors also found that individuals with increased SERCA activity reached lower T_b in torpor, while individuals with low proportions of LA in their sarcoplasmic reticulum membranes never actually entered torpor. This example illustrates that membrane remodeling in hibernators can greatly alter membrane-bound enzyme activity. Moreover, mitochondrial membrane remodeling has been reported in liver mitochondria throughout the stages of arousal from and entrance back into torpor in the thirteen-lined ground squirrel (Armstrong et al., 2011; Chung et al., 2011) and is a potential mechanism of regulation for BAT metabolic suppression. It is possible that the differential temperature sensitivity that I demonstrate represents a remodeling of mitochondrial membranes that allow BAT

mitochondria to function at low T_b during torpor, but these changes impair function at 37°C.

4.3 Mitochondrial membrane remodeling; a proposed mechanism for regulation of differential temperature sensitivity in BAT

The phospholipid composition of liver mitochondrial membranes changes during the transition from torpor to IBE (Armstrong and Staples, 2010; Armstrong et al., 2011; Chung et al., 2011). Armstrong et al. (2011) showed that phospholipid content changes in late arousal relative to IBE, while phospholipid polyunsaturated fatty acid content decreased throughout arousal in liver mitochondrial membranes. Liver mitochondrial respiration showed a significant positive correlation with mitochondrial phospholipid content of palmitoleic acid (16:1), a relatively minor monounsaturated fatty acid (Armstrong et al., 2011). Increased amounts of 16:1 in liver mitochondrial membranes has been linked with elevated CPT1 activity and diminished sensitivity of CPT1 to malonyl-CoA, a CPT1 inhibitor (Power et al., 1994). In BAT, long chain fatty acyl-CoAs are the predominate substrates for powering thermogenesis via β-oxidation (Cannon and Nedergaard, 2004) and CPT1 activity differences could have profound effects on mitochondrial respiration rates via substrate availability limitations, especially because CPT1 and CPT2 are highly expressed during the hibernation season (Ballinger et al., 2016). In addition to substrate availability, 16:1 in the mitochondrial membrane may be involved in protecting critical membrane-bound proteins (e.g. ETS complexes) from oxidative damage. In cardiac mitochondria

from several bird species, 16:1 content is positively correlated with body mass and maximum life span and is less susceptible to oxidative damage compared to polyunsaturated fatty acids (Gutiérrez et al., 2009). This is relevant to my results because reactive oxygen species production increases during arousal from torpor in arctic ground squirrels (Tøien et al., 2001), and thus an increase in 16:1 in BAT mitochondrial membrane phospholipids may help to diminish oxidative damage to membrane structure and enzyme function.

Diversity in fatty acid chain length and unsaturation also contributes to the diversity of mitochondrial membrane phospholipids, which is essential for the biophysical properties of the membrane (MacDonald and Sprecher, 1991; Schlame and Ren, 2006). Additionally, activities of enzymes in the inner mitochondrial membrane are dependent on acyl chain remodeling. For example, impairment of the remodeling of cardiolipin (CL), which represents a large proportion of polar lipids in the mitochondrial membrane (Armstrong et al., 2011), may disrupt the assembly and stability of the ETS enzymes (Schlame and Ren, 2006). Typically, acyl chain remodeling involves the phospholipase A family (PLAs), which catalyze the removal of an acyl chain from glycerol, and transacylases that replace them with a different fatty acyl chain (MacDonald and Sprecher, 1991; Shindou et al., 2009). CL remodeling has been extensively investigated in humans due to its important role in mitochondrial function and disease (Chicco and Sparagna, 2007). CL remodeling involves tafazzin, a transacylase localized to the mitochondrial membranes that creates a specific arrangement of CL species (Malhotra et al., 2009; Xu et al., 2009). Deficiency of

48

tafazzin alters CL composition and is related to dramatic changes in mammalian mitochondrial morphology and exercise capacity (Powers et al., 2013; Vreken et al., 2000). If tafazzin or PLAs were differentially regulated in torpor and IBE, this would likely have significant effects on the thermogenic capacity of BAT mitochondria.

If any or all of these changes occur in BAT mitochondria, they would likely affect the activity of the ETS enzymes *in situ*. These effects, however, would not be reflected in my spectrophotometric enzyme assays, as the mitochondria were lysed and homogenized, removing the enzymes from their native state. These effects would also not be reflected in the adipocyte respiration, where the cells were kept at warm temperatures during the lengthy isolation process, potentially allowing membrane remodeling enzymes ample time and favourable temperatures to reverse any changes. However, these regulatory mechanisms would still be apparent in the intact organelle respiration, as the mitochondrial isolation protocol occurs entirely at low temperatures (4°C) and homogenization and centrifugation rapidly separate mitochondria from the cytosolic components responsible for the remodeling. I suggest, therefore, that the isolated mitochondria likely better represent the "native" metabolic state of BAT than the isolated adipocyte.

4.4 Conclusions and future directions

My findings show that there is differential temperature sensitivity of BAT mitochondrial respiration between IBE and torpor, which would facilitate BAT

49

thermogenesis at the low T_b experienced early in arousal. For instance, the T_b of a squirrel as it begins the transition into IBE is ~5°C and yet the BAT is still activated and begins rapid thermogenesis even at this cold, unfavourable temperature to warm the rest of the body to 37°C.

I attempted to discern the mechanism underlying these temperature sensitivity differences by examining individual ETS enzyme activities. I found that when removed from their native state in the intact organelle, the trends seen in the intact mitochondria respirometry were not reflected in ETS enzyme complexes. To better understand how these results translated to higher levels of organization, I isolated intact BAT adipocytes from torpid and IBE ground squirrels but found that the long isolation process likely altered the trends seen in earlier mitochondrial experiments.

Future work should include membrane composition studies that examine the changes in phospholipid head group abundance and fatty acid unsaturation between torpor and IBE (similar to those that have been previously conducted on liver mitochondria by members of my lab). These studies would allow investigation of the changes, if any, in BAT mitochondrial membrane composition throughout a torpor-arousal cycle. Since the metabolic suppression happens rapidly during entrance (at warm T_b), while the reversal of the suppression occurs slowly during arousal from torpor (at cold T_b), these changes are likely enzyme mediated and follow Q_{10} kinetics. Accordingly, future experiments could also involve developing a new adipocyte isolation protocol, possibly using inhibitor cocktails for mitochondrial membrane remodeling

enzymes (e.g. tafazzin and PLAs) to assess this as a potential regulator of BAT adipocyte and mitochondrial respiration during arousal and entrance. This may prove to be logistically difficult because arousals are difficult to predict and any inhibitors must cross the plasma membrane and must not inhibit any enzymes involved in metabolism. Nevertheless, my project leaves many doors open for future work in elucidating the mechanisms associated with the temperature sensitivity and activity of BAT during hibernation.

REFERENCES

Armstrong, C. and Staples, J. F. (2010). The role of succinate dehydrogenase and oxaloacetate in metabolic suppression during hibernation and arousal. *J. Comp. Physiol. B.* **180**, 775–783.

Armstrong, C., Thomas, R. H., Price, E. R., Guglielmo, C. G. and Staples, J. F. (2011). Remodeling mitochondrial membranes during arousal from hibernation. *Physiol. Biochem. Zool.* **84**, 438–449.

Ballinger, M. A., Hess, C., Napolitano, M. W., Bjork, J. A. and Andrews, M. T. (2016). Seasonal Changes in Brown Adipose Tissue Mitochondria in a Mammalian Hibernator: from Gene Expression to Function. *Am. J. Physiol. Regul. Integr. Comp. Physiol.* ajpregu.00463.2015.

Barger, J. L., Brand, M. D., Barnes, B. M. and Boyer, B. B. (2003). Tissue-specific depression of mitochondrial proton leak and substrate oxidation in hibernating arctic ground squirrels. *Am. J. Physiol. Regul. Integr. Comp. Physiol.* **284**, R1306-13.

Bradford, M. M. (1976). A rapid and sensitive method for the quantitation of microgram quantities of protein utilizing the principle of protein-dye binding. *Anal. Biochem.* **72**, 248–54.

Brown, J. C. L. and Staples, J. F. (2014). Substrate-specific changes in mitochondrial respiration in skeletal and cardiac muscle of hibernating thirteen-lined ground squirrels. *J. Comp. Physiol. B.* **184**, 401–414.

Brown, J. C. L., Chung, D. J., Belgrave, K. R. and Staples, J. F. (2012).

Mitochondrial metabolic suppression and reactive oxygen species production in liver and skeletal muscle of hibernating thirteen-lined ground squirrels. *Am. J. Physiol. Regul. Integr. Comp. Physiol.* **302**, R15-28.

Brown, J. C. L., Chung, D. J., Cooper, A. N. and Staples, J. F. (2013). Regulation of succinate-fuelled mitochondrial respiration in liver and skeletal muscle of hibernating thirteen-lined ground squirrels. *J. Exp. Biol.* **216**, 1736–43.

Brustovetsky, N. N., Mayevsky, E. I., Grishina, E. V, Gogvadze, V. G. and Amerkhanov, Z. G. (1989). Regulation of the rate of respiration and oxidative phosphorylation in liver mitochondria from hibernating ground squirrels, Citellus undulatus. *Comp. Biochem. Physiol. B*. **94**, 537–41.

Cameron, I. L. and Smith, R. E. (1964). Cytological responses of brown fat tissue in cold-exposed rats. *J. Cell Biol.* **23**, 89–100.

Cannon, B. (1968). Oxidative Metabolism in Cells Isolated from Brown Adipose Tissue 1 . Catecholamine and Fatty Acid Stimulation of Respiration. **i**, 15–22.

Cannon, B. (1977). The mitochondrial ATPase of brown adipose tissue; Purification and Comparison with the Mitochondrial ATPase from Beef Heart. *FEBS Lett.* **76**, 284–289.

Cannon, B. and Nedergaard, J. (2004). Brown Adipose Tissue : Function and Physiological Significance. 277–359.

Cannon, B. and Nedergaard, J. (2008). Studies of thermogenesis and mitochondrial function in adipose tissues. *Methods Mol. Biol.* **456**, 109–21.

Chicco, A. J. and Sparagna, G. C. (2007). Role of cardiolipin alterations in mitochondrial dysfunction and disease. *Am. J. Physiol. Cell Physiol.* **292**, C33-44.

Chung, D., Lloyd, G. P., Thomas, R. H., Guglielmo, C. G. and Staples, J. F. (2011). Mitochondrial respiration and succinate dehydrogenase are suppressed early during entrance into a hibernation bout, but membrane remodeling is only transient. *J. Comp. Physiol. B.* **181**, 699–711.

Chung, D. J., Szyszka, B., Brown, J. C. L., Hüner, N. P. and Staples, J. F. (2013). Changes in the mitochondrial phosphoproteome during mammalian hibernation. *Physiol. Genomics* **45**, 389–399.

Else, P. L. and Hulbert, A. J. (1981). Comparison of the "mammal machine" and the "reptile machine": energy production. *Am. J. Physiol.* **240**, R3-9.

Else, P. L. and Wu, B. J. (1999). What role for membranes in determining the higher sodium pump molecular activity of mammals compared to ectotherms? *J Comp Physiol B* **169**, 296–302.

Giroud, S., Frare, C., Strijkstra, A., Boerema, A., Arnold, W. and Ruf, T. (2013). Membrane Phospholipid Fatty Acid Composition Regulates Cardiac SERCA Activity in a Hibernator, the Syrian Hamster (Mesocricetus auratus). *PLoS One* **8**, e63111.

Gutiérrez, A. M., Reboredo, G. R., Mosca, S. M. and Catalá, A. (2009). High resistance to lipid peroxidation of bird heart mitochondria and microsomes: Effects of mass and maximum lifespan. *Comp. Biochem. Physiol. A. Mol. Integr. Physiol.* **154**, 409–16.

Hampton, M., Melvin, R. G. and Andrews, M. T. (2013). Transcriptomic analysis of brown adipose tissue across the physiological extremes of natural hibernation. *PLoS One* **8**, 1–12.

Heller, H. C. (1986). *Living in the cold: physiological and biochemical adaptations : proceedings of the Seventh International Symposium on Natural Mammalian Hibernation, held October 6-11, 1985, at the Stanford University Conference Center, Fallen Leaf Lake, California, U.S.A*. Elsevier.

Hemmingsen, A. (1960). Energy metabolism as related to body size and respiratory surfaces, and its evolution. *Reports Steno Meml. Hosp. Nord. Insul. Lab.* **9**, 1–110.

Hochachka, P. P. W. and Somero, G. N. (2002). *Biochemical Adaptation: Mechanism and Process in Physiological Evolution*.

Kerner, J. and Hoppel, C. (2000). Fatty acid import into mitochondria. *Biochim. Biophys. Acta* **1486**, 1–17.

Kirby, D. M., Thorburn, D. R., Turnbull, D. M. and Taylor, R. W. (2007). Biochemical Assays of Respiratory Chain Complex Activity. *Methods Cell Biol.* **80**, 93–119.

Kleiber, M. (1961). *The fire of life: an introduction to animal energetics*. Wiley.

Lovegrove, B. G. (2012). The evolution of endothermy in Cenozoic mammals: a plesiomorphic-apomorphic continuum. *Biol. Rev. Camb. Philos. Soc.* **87**, 128–62.

MacDonald, J. I. and Sprecher, H. (1991). Phospholipid fatty acid remodeling in mammalian cells. *Biochim. Biophys. Acta* **1084**, 105–21.

Malhotra, A., Xu, Y., Ren, M. and Schlame, M. (2009). Formation of molecular species of mitochondrial cardiolipin. 1. A novel transacylation mechanism to shuttle fatty acids between sn-1 and sn-2 positions of multiple phospholipid species. *Biochim. Biophys. Acta* **1791**, 314–20.

Mathers, K. E., McFarlane, S. V., Zhao, L. and Staples, J. F. Regulation of mitochondrial metabolism during hibernation by reversible suppression of electron transport system enzymes. *J. Comp. Physiol. B.*

McGarry, J. D. and Brown, N. F. (1997). The Mitochondrial Carnitine Palmitoyltransferase System - From Concept to Molecular Analysis. *Eur. J. Biochem.* **244**, 1–14.

Milner, R. E., Wang, L. C. and Trayhurn, P. (1989). Brown fat thermogenesis during hibernation and arousal in Richardson's ground squirrel. *Am. J. Physiol.* **256**, R42-8.

Muleme, H. M., Walpole, A. C., Staples, J. F., Physiological, S., Zoology, B. and June, N. M. (2006). Mitochondrial Metabolism in Hibernation : Metabolic Suppression , Temperature Effects , and Substrate Preferences. *Physiol. Biochem. Zool.* **79**, 474–483.

Nedergaard, J. and Cannon, B. (1984). Preferential utilization of brown adipose tissue lipids during arousal from hibernation in hamsters. *Am. J. Physiol.* **247**, R506–R512.

Pande, S. V (1975). A mitochondrial carnitine acylcarnitine translocase system. *Proc. Natl. Acad. Sci. U. S. A.* **72**, 883–7.

Pearson, O. P. (1947). The Rate of Metabolism of Some Small Mammals.

Ecology **28**, 127–145.

Pehowich, D. J., Macdonald, P. M., McElhaney, R. N., Cossins, A. R. and Wang, L. C. (1988). Calorimetric and spectroscopic studies of lipid thermotropic phase behavior in liver inner mitochondrial membranes from a mammalian hibernator. *Biochemistry* **27**, 4632–8.

Power, G. W., Yaqoob, P., Harvey, D. J., Newsholme, E. A. and Calder, P. C. (1994). The effect of dietary lipid manipulation on hepatic mitochondrial phospholipid fatty acid composition and carnitine palmitoyltransferase I activity. *Biochem. Mol. Biol. Int.* **34**, 671–84.

Powers, C., Huang, Y., Strauss, A. and Khuchua, Z. (2013). Diminished Exercise Capacity and Mitochondrial bc1 Complex Deficiency in Tafazzin-Knockdown Mice. *Front. Physiol.* **4**, 74.

Schlame, M. and Ren, M. (2006). Barth syndrome, a human disorder of cardiolipin metabolism. *FEBS Lett.* **580**, 5450–5.

Scholander, P. F., Flagg, W., Walters, V. and Irving, L. (1953). Climatic Adaptation in Arctic and Tropical Poikilotherms. *Physiol. Zool.* **26**, 67–92.

Shabalina, I. G., Vrbacký, M., Pecinová, A., Kalinovich, A. V, Drahota, Z., Houštěk, J., Mráček, T., Cannon, B. and Nedergaard, J. (2014). ROS production in brown adipose tissue mitochondria: The question of UCP1-dependence. *Biochim. Biophys. Acta* **1837**, 2017–2030.

Shindou, H., Hishikawa, D., Harayama, T., Yuki, K. and Shimizu, T. (2009). Recent progress on acyl CoA: lysophospholipid acyltransferase research. *J. Lipid Res.* **50 Suppl**, S46-51.

Snapp, B. D. and Heller, H. C. (1981). Suppression of Metabolism during Hibernation in Ground Squirrels (Citellus lateralis). *Physiol. Zool.* **54**, 297–307.

Staples, J. F. (2016). Metabolic Flexibility: Hibernation, Torpor, and Estivation. In *Comprehensive Physiology*, p. John Wiley & Sons, Inc.

Staples, J. F. and Hochachka, P. W. (1997). Liver energy metabolism during hibernation in the golden-mantled ground squirrel, Spermophilus lateralis. *Can. J. Zool.* **75**, 1059–1065.

Takaki, M., Nakahara, H., Kawatani, Y., Utsumi, K. and Suga, H. (1997). No suppression of respiratory function of mitochondrial isolated from the hearts of anesthetized rats with high-dose pentobarbital sodium. *Jpn. J. Physiol.* **47**, 87–92.

Tøien Ø, Drew, K. L., Chao, M. L. and Rice, M. E. (2001). Ascorbate dynamics and oxygen consumption during arousal from hibernation in Arctic ground squirrels. *Am. J. Physiol. Regul. Integr. Comp. Physiol.* **281**, R572-83.

Vaughan, D. K., Gruber, A. R., Michalski, M. L., Seidling, J. and Schlink, S. (2006). Capture, care, and captive breeding of 13-lined ground squirrels, Spermophilus tridecemlineatus. *Lab Anim. (NY).* **35**, 33–40.

Vreken, P., Valianpour, F., Nijtmans, L. G., Grivell, L. A., Plecko, B., Wanders, R. J. and Barth, P. G. (2000). Defective remodeling of cardiolipin and phosphatidylglycerol in Barth syndrome. *Biochem. Biophys. Res. Commun.* **279**, 378–82.

Xu, Y., Zhang, S., Malhotra, A., Edelman-Novemsky, I., Ma, J., Kruppa, A., Cernicica, C., Blais, S., Neubert, T. A., Ren, M., et al. (2009). Characterization of Tafazzin Splice Variants from Humans and Fruit Flies. *J. Biol. Chem.* **284**, 29230–29239.

Appendix A.   Animal use ethics approval

Western 🛡

2012-016::2:

AUP Number: 2012-016
AUP Title: Regulation of mitochondrial metabolism in mammalian hibernation and ageing.
Yearly Renewal Date: 08/01/2014

The YEARLY RENEWAL to Animal Use Protocol (AUP) 2012-016 has been approved, and will be approved for one year following the above review date.

1. This AUP number must be indicated when ordering animals for this project.
2. Animals for other projects may not be ordered under this AUP number.
3. Purchases of animals other than through this system must be cleared through the ACVS office.
   Health certificates will be required.

REQUIREMENTS/ COMMENTS
Please ensure that individual(s) performing procedures on live animals, as described in this protocol, are familiar with the contents of this document.

The holder of this Animal Use Protocol is responsible to ensure that all associated safety components (biosafety, radiation safety, general laboratory safety) comply with institutional safety standards and have received all necessary approvals. Please consult directly with your institutional safety officers.

Submitted by: Kinchlea, Will D
on behalf of the Animal Use Subcommittee

CURRICULUM VITAE

Name: Sarah McFarlane

Education: MSc Biology – 2016
University of Western Ontario

BSc Honors Double Major: Medical Science and Biology - 2014
University of Western Ontario

Scholarships: Queen Elizabeth II Graduate Scholarship in Science and Technology
2015

Awards: Helen I. Battle award at the Canadian Society of Zoologists Annual Meeting
2016 for best student poster presentation

Undergraduate Dean's Honor List
2012, 2013, 2014

Publications:

Mathers, K.E., **McFarlane, S.V**., Zhao, L., Staples, J.F. Regulation of
mitochondrial metabolism during hibernation by reversible suppression of
electron transport system enzymes. (in press, *J. Comp. Physiol. B*)

Presentations:

McFarlane, S.V., Mathers, K.E., Staples, J.F. 2015. Mitochondrial respiration in
brown adipose tissue of hibernating 13-lined ground squirrels, *Ictidomys
tridecemlineatus.* Canadian Society of Zoologists Annual Meeting, Calgary,
Alberta.

McFarlane S.V., Mathers, K.E., Staples, J.F. 2016. Reduced temperature
sensitivity of brown adipose tissue mitochondrial respiration during torpor.
Canadian Society of Zoologists Annual Meeting, London, Ontario.